A flavour of family symmetries in a family of flavour models

Adelhart Toorop, R. de

Chapter 4

The interplay between GUT and flavour symmetries in a Pati–Salam $\times$ S_4 model

> Il semble que la perfection soit atteinte non quand il n'y a plus rein à ajouter, mais quand il n'y a plus rein à retrancher.
>
> It seems that perfection is reached not when there is nothing more to add, but when there is nothing more to remove.
>
> *Antoine de Saint-Exupéry [98], Terre des Homes*

4.1 Introduction

In this chapter we investigate the possibility to combine flavour symmetries with Grand Unified Theory (GUT) symmetries. The desire to combine these two symmetries has three roots. Firstly, it is partly data-driven. There are structures that can be explained well by grand unified explanations and others that are well explained using flavour symmetries. As far as these concern the elementary masses, as a rule of thumb relations between the different family copies of a certain type of particle (e.g. charged leptons) can have explanations in family symmetries, while relations between different types of particles in one generation (e.g. the muon and the strange quark) might be explained by grand unified symmetries.

Secondly, there are aesthetic reasons to combine the two symmetries. Family symmetries reduce the number of fermionic representations by grouping particles of different families in single irreducible representations; grand unified symmetries do exactly the same with different particle types within a generation. Thirdly, there is the coincidence that in many models scale of family physics is close to the assumed GUT scale - see e.g. equation (2.86) and figure 1.14.

Flavour-GUT models have been constructed before, for references see e.g. [47]. In our opinion, these analyses emphasize the difficulty in the construction of a flavour GUT model which naturally lead to realistic fermion phenomenology and to a fair explanation of the gauge symmetry breaking chain to get $SU(3)_C \times U(1)_{em}$. In particular, the combinations of the constraints arising by the flavour symmetry and by the GUT group may lead to wrong predictions for the fermion masses and mixings. For instance if the lepton mixing is tribimaximal at the GUT scale and at leading order, it is not necessarily so at a low energy scale and to all orders in different perturbing parameters. The problem is usually avoided by recurring to non-minimal Higgs or flavon field content and by assuming peculiar symmetry breaking patterns of the GUT gauge symmetry and ascribing quite often at type-II seesaw as the origin of the neutrino masses. Moreover these patterns are often not supported by the study of the scalar Higgs potential, leaving open the question if such peculiar

patterns may be actually realized or not.

In this chapter we perform as complete an analysis as possible. The chapter is divided into three parts. The first part is introductory. In section 4.2, we list several patterns that can be seen in the mass sector and that may be explained by family symmetry pattern or GUT patterns. The section ends with a 'wishlist' of relations that the model we construct in the rest of the chapter should be able to reproduce. In section 4.3 we introduce the flavour part of the model and add some additional wishes to the list. Section 4.4 introduces the Pati–Salam GUT that the model in the next sections is based on.

In the second part, we construct the described model. Section 4.5 gives the contents of the model and in sections 4.6 and 4.7 we give the results respectively at leading order and next-to-leading order in the number of flavons inserted. Subleading effects are very important to obtain agreement with the data in models based on the bimaximal mixing pattern and we find that after section 4.7 all points of the wishlist are satisfied.

Section 4.8 is a bridge between the second and the third part of the chapter. In this section we show that the flavons used in sections 4.6 and 4.7 can indeed have the vacuum expectation values they are assumed to. This introduces extra complications as driving fields are needed, but this is not more than in the non-GUT model of Altarelli and Feruglio discussed in chapter 2.

In sections 4.9 and 4.10 we study respectively the Higgs alignment and the effects of renormalization group running. Here is becomes clear that the combination of flavour and GUT symmetries leads to unexpected interference effects. In fact some of the positive conclusions of the second part of the chapter have to be withdrawn.

Lastly, in section 4.11, we perform an analysis of the phenomenological consequences of our model on near-future neutrino experiments and in section 4.12 we present our conclusions.

4.2 A detailed look on patterns in the elementary fermion masses

In chapters 1 and 2 some patterns in the mass sector of the Standard Model were introduced. In section 1.4.1 we found that the masses in both quark sectors as well as in the charged lepton sector are highly hierarchical with comparable gaps between the third and second generation and the second and first generation on a logarithmic scale. In section 2.3.1 we discussed the Froggatt–Nielsen mechanism that can explain these structures in a natural way.

The model described in section 2.3.1 discusses only the charged lepton sector. Extension to the quark sector is obviously possible. From figure 1.16 we see that the gaps between the charged lepton and down quark states are comparable, while the gaps between the up quark states are clearly larger. The ratios between the muon and the tau mass and between the electron mass and the muon mass used in section 2.3.1 were λ^2 and λ^3 respectively, with $\lambda = 0.2$. This does also reasonably well describe the mass gaps in the down-type quark sector, although the strange quark is slightly too light. In the up-type quark sector, the gaps are larger and can be parameterized by ratios of λ^4 and λ^3 between the charm and the top and between the up and the charm respectively.

The other simplifying assumption in section 2.3.1 is the absence of off-diagonal terms. This is clearly not realistic. The presence of off-diagonal terms is necessary for the generation of mixing matrices. In the quark sector, where the mixing is relatively weak, the off-diagonal terms should be small. It is exactly the key point of the Froggatt–Nielsen mechanism to generate terms that are naturally small and in the model we study in this chapter, we show how we can use this at our convenience. To explain the larger mixing angles of the lepton sector, that might furthermore be close to special mixing patterns such as the tribimaximal or bimaximal one, the use of discrete non-Abelian flavour symmetries might be more appropriate.

While the Froggatt–Nielsen mechanism can provide relations between the ratios of masses of par-

ticles of the same type – charged leptons in the example of section 2.3.1 – it does not help much to explain patterns between particles of different type. Still, these relations might be present. A first hint might be given by the fact that the second (down-type quarks) and third line (charged leptons) in figure 1.16 are quite close together, allowing for the possibility of relations between charged lepton and down-type quark masses.

At low energy scales, such relations do not quite exist. For none of the three generations the charged lepton has the same mass as a quark or a simple multiple of it. When we discussed the Altarelli–Feruglio model in section 2.4, we found that flavour symmetries are often implemented at a high scale and that there are renormalization effects. If we run the renormalization group backwards we can evaluate the quark and lepton Yukawa couplings at a high scale and the corresponding masses are graphically depicted in figure 4.1. We find evidence for two relations. The first is bottom-tau unification

$$m_b = m_\tau. \tag{4.1}$$

The second relation goes by the name of the Georgi–Jarlskog relation [99] and it connects the muon mass with the mass of the strange quark

$$m_\mu = 3m_s \tag{4.2}$$

Both relations are supposed to hold at the scale of Grand Unification or slightly below. Given that this is far above the electroweak scale, the Higgs field does not have a vacuum expectation value here. The word 'mass', equal to the product of the relevant Yukawa coupling with the Higgs vev should thus be taken with a grain of salt. Technically, all particles are massless at this scale. What is meant is that the Yukawa couplings, evaluated at this scale, satisfy the given relations.

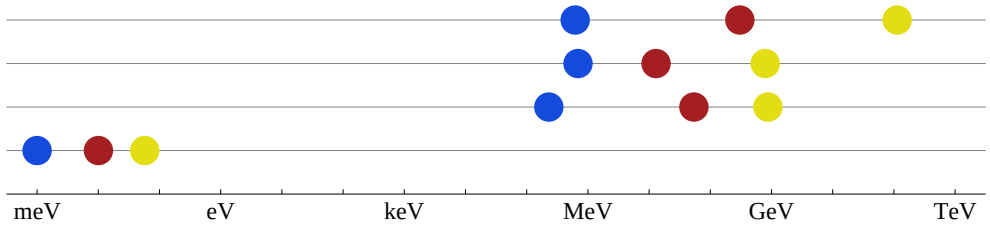

Figure 4.1: *The masses of the Standard Model fermions when evolved to a scale of* 10^{12} *GeV in the MSSM with tan* β *= 50 as discussed below.*

Lastly, we would like to explain the fact that the top quark is much heavier than the bottom quark and the tau lepton. In theories with more than one Higgs boson (for instance any supersymmetric theory), this may be explained by $\tan\beta$ or comparable quantities that give information about the relative vev of the Higgs that couples to the up- and down-sector. This large $\tan\beta$ itself should then follow from Higgs physics.

In table 4.1 we summarize the results mentioned in this section: the table contains the masses of the quarks and charged leptons at the scale of their own mass (or, if this is unavailable, at 2 GeV). The table also gives the masses at a high energy scale calculated in [100] using the renormalization group running of the MSSM with large $\tan\beta = 50$. We choose a value of 10^{12} GeV for the high energy scale. In section 4.9 we find that this is indeed close to the relevant scale for the generation of fermion masses.

The errors for the quarks are rather large, but the bottom-tau unification and the Georgi–Jarlskog relation are realized well within the margins of error. We also show ratios of the small Yukawa couplings with certain powers of $\lambda = 0.2$ such that the resulting couplings are of order 1. As a note of caution, we mention that the specific value of the high scale and of $\tan\beta$ are both slightly arbitrary and that the model inspired by the relations in the table does not have the MSSM as low energy limit. Therefore we perform a simple one-loop renormalization analysis in section 4.10.

As mentioned in chapter 2, not many parameters of the neutrino masses are known. It will be the aim of a family symmetric model to reproduce the solar and atmospheric mass differences of table 2.3.

	Generation 1	Generation 2	Generation 3
Charged Leptons	$m_e(m_e) = 0.51\,\text{MeV}$ $m_e(10^{12}\text{GeV}) = 0.23\,\text{MeV}$ $y_e(10^{12}\text{GeV}) = 6.6 \times 10^{-5}$ $y_e(10^{12}\text{GeV})/\lambda^6 = 1.0$	$m_\mu(m_\mu) = 106\,\text{MeV}$ $m_\mu(10^{12}\text{GeV}) = 54\,\text{MeV}$ $y_\mu(10^{12}\text{GeV}) = 0.016$ $y_\mu(10^{12}\text{GeV})/\lambda^3 = 1.9$	$m_\tau(m_\tau) = 1.78\,\text{GeV}$ $m_\tau(10^{12}\text{GeV}) = 875\,\text{MeV}$ $y_\tau(10^{12}\text{GeV}) = 0.25$ $y_\tau(10^{12}\text{GeV})/\lambda = 1.25$
Down-type Quarks	$m_d(2\text{GeV}) = 5.0 \pm 2.0\,\text{MeV}$ $m_d(10^{12}\text{GeV}) = 0.69^{+0.31}_{-0.29}\,\text{MeV}$ $y_d(10^{12}\text{GeV}) = \left(2.0^{+0.9}_{-0.8}\right) \times 10^{-4}$ $y_d(10^{12}\text{GeV})/\lambda^6 = 3.1^{+1.4}_{-1.3}$	$m_s(2\text{GeV}) = 95 \pm 25\,\text{MeV}$ $m_s(10^{12}\text{GeV}) = 13 \pm 4\,\text{MeV}$ $y_s(10^{12}\text{GeV}) = \left(3.7 \pm 1.2\right) \times 10^{-3}$ $y_s(10^{12}\text{GeV})/\lambda^3 = 0.46 \pm 0.14$	$m_b(m_b) = 4.20 \pm 0.07\,\text{GeV}$ $m_b(10^{12}\text{GeV}) = 0.79^{+0.05}_{-0.04}\,\text{GeV}$ $y_b(10^{12}\text{GeV}) = 0.22^{+0.01}_{-0.01}$ $y_b(10^{12}\text{GeV})/\lambda = 1.14^{+0.07}_{-0.05}$
Up-type Quarks	$m_u(2\text{GeV}) = 2.2^{+0.8}_{-0.7}\,\text{MeV}$ $m_u(10^{12}\text{GeV}) = 0.62^{+0.26}_{-0.22}\,\text{MeV}$ $y_u(10^{12}\text{GeV}) = \left(3.6^{+1.5}_{-1.3}\right) \times 10^{-6}$ $y_u(10^{12}\text{GeV})/\lambda^8 = 1.4^{+0.6}_{-0.5}$	$m_c(m_c) = 1.25 \pm 0.09\,\text{GeV}$ $m_c(10^{12}\text{GeV}) = 0.304^{+0.046}_{-0.045}\,\text{GeV}$ $y_c(10^{12}\text{GeV}) = \left(1.7 \pm 0.3\right) \times 10^{-3}$ $y_c(10^{12}\text{GeV})/\lambda^5 = 5.5 \pm 0.8$	$m_t(m_t) = 162.9 \pm 2.8\,\text{GeV}$ $m_t(10^{12}\text{GeV}) = 113.2^{+8.9}_{-7.7}\,\text{GeV}$ $y_t(10^{12}\text{GeV}) = 0.65^{+0.05}_{-0.04}$ $y_t(10^{12}\text{GeV})/\lambda = 3.2^{+0.3}_{-0.2}$

Table 4.1: *Parameters of quark and charged lepton masses evaluated at low scales and at a scale of* 10^{12} *GeV, calculated in [100] in the MSSM with* $\tan\beta = 50$*. For the charged leptons no error bars are given. In principle, their values are known to much higher precision. This extra information is not useful, as model dependent choices (e.g. the exact value of* $\tan\beta$*) bring in much more uncertainty.*

The actual neutrino masses themselves and in particular their ordering should then be a prediction of the specific model.

We conclude this section with a 'wishlist' of properties of the masses of quarks and leptons that a complete model should be able to reproduce:

- Find the right masses for the third family, in particular the large top mass.
- Suppress the second family masses: $m_\mu/m_\tau = m_s/m_b = \lambda^2$ and $m_c/m_t = \lambda^4$.
- Suppress the first family masses even stronger: $m_e/m_\tau = m_d/m_b = \lambda^5$ and $m_u/m_t = \lambda^7$.
- Reproduce the bottom-tau and strange-muon relations.
- Reproduce the atmospheric and solar mass differences
- Predict the absolute neutrino mass scale and the neutrino hierarchy.

Next to properties of the masses, we would also like to reproduce or predict properties of the mixings of the elementary fermions. The choices of our model regarding mixing are discussed in the next section.

4.3 Bimaximal versus tribimaximal mixing

At the end of section 2.4 we discussed the next-to-leading order (NLO) corrections to the Altarelli–Feruglio model, or rather to a simple extension of it that contains quarks. The leading order (LO) results of this model were exact tribimaximal mixing in the lepton sector and no mixing at all in the quark sector. We mentioned that these leading order mixing patterns were very accurate in the neutrino sector, perhaps even too accurate. The measured value of the solar mixing angle is very close to the tribimaximal value. The deviations can be at most of order λ^2, where λ is still defined as a parameter with value 0.2. The measurement error for the atmospheric mixing angle is rather large, but also here the central value agrees very well with the tribimaximal prediction and corrections no larger than of order λ^2 are favoured. The size of corrections in the (1 2) and (2 3) sector naturally imply very small corrections to the reactor mixing angle. This angle was zero at leading order and thus θ_{13}^l very close to zero is a prediction of the model – one that is in contradiction with the latest data. In the Wolfenstein picture, the parameter λ is defined as the size of the Cabibbo angle. If the LO result has no quark mixing, this should all be generated at NLO, thus requiring much larger corrections in the quark than in the lepton sector.

As described in section 2.4 NLO terms contain an extra flavon with respect to the leading order. We recall that the suppression of NLO terms is v_X/Λ with v_X the vev of any flavon and Λ the cut-off scale of the model. In models that have zero quark mixing at leading order and that reproduce the Cabibbo angle at the NLO, we thus need

$$\frac{v_X}{\Lambda} \approx \lambda = 0.2. \tag{4.3}$$

Good care must be taken to ensure that the two other mixing angles of the CKM matrix do not obtain values as large as the Cabibbo angle, but in general it is possible to have these vanishing also at NLO and to produce them only at the next-to-next-to-leading order. See also figure 4.2.

It is clear that the size of NLO corrections $v_X/\Lambda \approx 0.2$ is incompatible with the $v_X/\Lambda \lesssim 0.05$ found at the end of section 2.4 from lepton considerations. Now there are three possibilities. The first option entails a complete separation of the flavon-induced physics of the quark and lepton sectors. Instead of one value of v_X/Λ, there are separate values for v_{X_q}/Λ (large) and v_{X_l}/Λ (small). These two values of the flavon vevs might come from flavons that barely talk to each other or even from different symmetry groups in the two sectors. Obviously, the idea of separating the flavour aspects

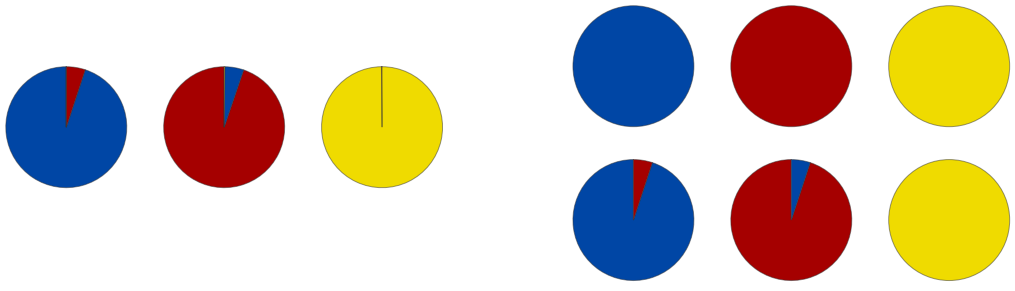

Figure 4.2: *Left: pie charts showing the flavour content of the three quark eigenstates. Right: the no-mixing predictions of a typical flavour model at LO (upper line) and a NLO result, where θ_{12} is corrected to the size of the observed Cabibbo angle. The other two mixing angles follow at higher orders, hence the absence of the red sliver in the third mass eigenstate (lower line).*

of quark and lepton physics is badly compatible with the concept of a unified description of the two sectors as discussed in the next section.

In both other options a single value of $v_X/\Lambda \approx 0.2$ is assumed. In a second scenario, the couplings of flavons to the Yukawa terms are tailored such that only in the quark sector there is a correcting term with just one extra flavon (thus giving a large correction), while in the lepton sector, the first correcting term has two extra flavons, leading to a much smaller correction of order $(v_X/\Lambda)^2$. This tailoring is highly non-trivial and might require the addition of more than one additional Z_n symmetry.

Thirdly, one can accept large corrections in both the quark and the lepton sector. In that case, however, the tribimaximal mixing pattern is not a good leading order result, as the near-perfect agreement with the data gets completely destroyed at the NLO. This is graphically shown in figure 4.3.

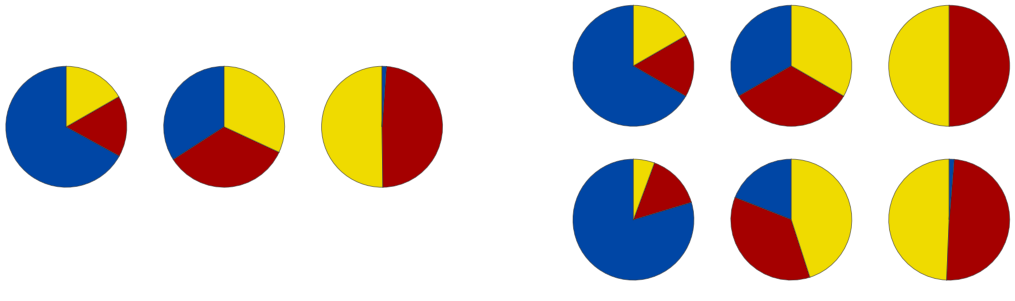

Figure 4.3: *Left: pie charts showing the flavour content of the three neutrino eigenstates. Right: The tribimaximal mixing pattern (upper line) and a possible NLO result if corrections of the size λ are allowed. We have used $\delta\theta^l_{12} = -0.7\theta_C$, $\delta\theta^l_{13} = 0.5\theta_C$. The (2 3) angle is not corrected. This is indeed the case in some models and allows for a more fair comparison with figure 4.4*

The fact that the quark sector requires a relatively large NLO correction, seems to suggest a lepton mixing pattern that also requires large corrections, i.e. one that at leading order described the data less perfect than the tribimaximal pattern. An interesting new piece of evidence are the so-called quark-lepton complementarity relations.

$$\theta^l_{12} + \theta^q_{12} \simeq \pi/4 + \mathcal{O}(\lambda^2)\,, \qquad \theta^l_{23} + \theta^q_{23} \simeq -\pi/4 + \mathcal{O}(\lambda^2)\,. \tag{4.4}$$

We note that there does not seem to be such a relation between the (1 3)-angles. In the quark sector, this angle is tiny (of the order of λ^3); in the lepton sector, the T2K result points to a value slightly

smaller than λ. There is certainly no angle close to $\pi/4$ involved. The complementarity relations point at a description in which the quark and lepton mixing angles are not only related by being part of a powerseries with a comparable expansion parameter (v_X/Λ), but may even be connected even stronger. In the next section we discuss the grand unified model of Pati and Salam, in which there is indeed a strong relationship between quark and lepton mass matrices as leptons may be seen as the fourth colour. In minimal Pati–Salam models one finds equal mass matrices for charged leptons and down-type quarks

$$M_e = M_d \ . \tag{4.5}$$

This obviously implies a common source for the mixing angles. The model described in this chapter is not a minimal Pati–Salam model and there are significant corrections to equation (4.5), but the idea of a common source for quark and lepton mixing angles remains.

The bimaximal pattern of section 3.3.2 is a candidate mixing pattern that matches the criteria above[1]. At leading order, both the (1 2) and (2 3) mixing angles in the lepton sector are maximal (45°), while the third lepton mixing angle as well as all quark mixing angles are zero. An elaborate model [64] exists in the literature where bimaximal mixing in the lepton sector is derived from a S_4 discrete symmetry. Our model can be seen as an revision of [64] in order to include a realistic description of the quark sector.

One way to realize bimaximal mixing at leading order is now if the neutrino mass matrix is diagonalized by a maximal angle in the (1 2) sector[2], while for all charged particles (that is, charged leptons and both types of quarks), the mixing is maximal in the (2 3) sector. Writing a rotation in the (i j) plane of a mass matrix over an angle α as $R_{ij}(\alpha)$, we get

$$\begin{aligned} V_{\text{CKM}} &= (V_L^u)^\dagger V_L^d = R_{23}(-\frac{\pi}{4}) \times R_{23}(\frac{\pi}{4}) = \mathbb{1} \\ V_{\text{PMNS}} &= (V_L^e)^\dagger V^\nu = R_{23}(-\frac{\pi}{4}) \times R_{12}(\frac{\pi}{4}) \ . \end{aligned} \tag{4.6}$$

These maximal mixing angles can originate from mass matrices that are relatively simple; they have many zeroes in the elements we do not want to get mixed. In this chapter, we choose the following realization for the neutrino mass matrix at leading order[3]

$$M^\nu \propto \begin{pmatrix} k_0 & k_1\lambda & 0 \\ k_1\lambda & k_0 & 0 \\ 0 & 0 & k_0 \end{pmatrix} \ . \tag{4.7}$$

The charged particle mass matrices (generically denoted as M^x) are given at leading order by

$$M^x \propto \begin{pmatrix} 0 & 0 & 0 \\ 0 & y_b & y_a \\ 0 & -y_b & y_a \end{pmatrix} \quad \rightarrow \quad M^x (M^x)^\dagger \propto \begin{pmatrix} 0 & 0 & 0 \\ 0 & y_a^2 + y_b^2 & y_a^2 - y_b^2 \\ 0 & y_a^2 - y_b^2 & y_a^2 + y_b^2 \end{pmatrix} \ . \tag{4.8}$$

Here, y_a will eventually be leading in the generation of the third generation masses and y_b in those of the second generation. The relative smallness of the second generation masses is explained by a positive Froggatt–Nielsen charge; y_b should therefore not be read as a true parameter of the model, but rather as an effective parameter after 'dilution' by the Froggatt–Nielsen mechanism[4]. At this

[1] It is amusing to see that the first references to the bimaximal mixing pattern are some four years older than those to the tribimaximal mixing pattern. From a modern point of view, the tribimaximal pattern is more natural since already at first order it reproduces decent agreement with the data. Obviously, this was not known in the first years of neutrino oscillations. As long as the solar mixing angle were in agreement with an maximal angle, the bimaximal pattern was considered a good leading order fit; when it was found that θ_{12}^l is significantly smaller than 45°, it was dismissed for a while. Approximately ten years after its first postulation, the pattern re-emerged as a pattern feasible with large next-to-leading order effects

[2] We recall that the CKM and PMNS matrix are respectively defined as $V_{\text{CKM}} = (V_L^u)^\dagger V_L^d$ and $V_{\text{PMNS}} = (V_L^e)^\dagger V^\nu$, where V^ν is the matrix that appears in the diagonalization of the neutrinos (2.44) and V_L^x, $x \in \{u, d, e\}$ are the matrices that diagonalize $M^x M^{x\,\dagger}$.

[3] The appearance of λs in this formula makes it look like a NLO expression instead of a LO result. However, the matrix with just the k_0 elements is proportional to the identity and does not allow the determination of V^ν as it is invariant under the action of any unitary matrix.

[4] This implies again that some terms in the mass matrix are larger than others; this choice follows from consistent qualification of LO and NLO effects.

level of approximation, the first generation particles are still massless; their masses are generated by higher order effects.

At next-to-leading-order, the Cabibbo angle should be reproduced in the quark sector, while keeping the two other mixing angles small. In the lepton sector, there should be a large correction to the (1 2) mixing angle. The (2 3) angle should not be corrected at this order, as the data suggest at most a λ^2 deviation from the maximal value. From the input-side, there is no preference for a specific behaviour of the (1 3) mixing angle. In our model, the correction is large, of order λ. This is good news in view of the latest data.

This pattern of NLO corrections can be generated as follows. In the neutrino mass matrix (4.7), the only correction is in the (3 3) element

$$(M^\nu) \propto \begin{pmatrix} k_0 & k_1\lambda & 0 \\ k_1\lambda & k_0 & 0 \\ 0 & 0 & k_0 + k_2\lambda^2 \end{pmatrix} . \tag{4.9}$$

This is still diagonalized by $R_{12}(\frac{\pi}{4})$. In the charged sector, NLO terms should give non-zero elements in the (1 2) and (1 3) elements, but not in the first column.

$$M^x \propto \begin{pmatrix} 0 & y_d\lambda & y_c\lambda \\ 0 & y_b & y_a \\ 0 & -y_b & y_a \end{pmatrix} \quad \rightarrow \quad M^x(M^x)^\dagger \propto \begin{pmatrix} 0 & (y_a y_c - y_b y_d)\lambda & (y_a y_c + y_b y_d)\lambda \\ (y_a y_c - y_b y_d)\lambda & y_a^2 + y_b^2 & y_a^2 - y_b^2 \\ (y_a y_c + y_b y_d)\lambda & y_a^2 - y_b^2 & y_a^2 + y_b^2 \end{pmatrix} . \tag{4.10}$$

This is diagonalized by a combination of rotations over all three mixing angles

$$V_L^x = R_{23}(\frac{\pi}{4}).R_{13}(f\lambda).R_{12}(g\lambda) . \tag{4.11}$$

Here, f and g are functions of the parameters of the mass matrix and we ignored complex phases. It is easy to see that in the diagonalization of the mass matrices in (4.10), the $(1\ 2)$ rotation originates dominantly from the second families, while the $(1\ 3)$ rotation comes from the third families. The parameters y_a, y_b, y_c, y_d in equation (4.10) generically stand for parameters in the mass matrices of all three types of charged particles.

In our model, the parameters y_a and y_c are universal for up quarks, down quarks and charged leptons, while y_b and y_d are the same for e and d, but different for u. This relates to the fact that the hierarchy is larger in the up sector than in the two other sectors. The Higgs content of our model is such that the coupling that gives mass to the second generation charged leptons and down-type quarks does not have an analogue for the up-type quarks. The mass of the charm quark eventually follows from a term whose d and e analogue is subleading. This has two positive consequences. Firstly that the mass gap between top and charm is indeed larger than between the bottom and the strange and between the tau lepton and the muon. Secondly that the parameter f of equation (4.11) is the same for all three types of particles, while g is the same for charged leptons and down quarks, but different for up quarks.

$$f = f_e = f_d = f_u$$

$$g_e = g_d \neq g_u$$

The mixing matrices at next-to-leading order read

$$\begin{aligned} V_{\text{PMNS}} = (V_L^e)^\dagger V^\nu =& \Big[R_{12}(-g_e\lambda)R_{13}(-f\lambda)R_{23}\big(-\frac{\pi}{4}\big)\Big]R_{12}\big(\frac{\pi}{4}\big) \\ =& R_{23}\big(-\frac{\pi}{4}\big)R_{13}(\tilde{f}\lambda)R_{12}\big(\frac{\pi}{4} - \tilde{g}_e\lambda\big) , \\ V_{\text{CKM}} = (V_L^u)^\dagger V_L^d =& \Big[R_{12}(-g_u\lambda)R_{13}(-f\lambda)R_{23}\big(-\frac{\pi}{4}\big)\Big]\Big[R_{23}\big(\frac{\pi}{4}\big)R_{13}(f\lambda)R_{12}(g_d\lambda)\Big] \\ =& R_{12}\big((g_d - g_u)\lambda\big) . \end{aligned} \tag{4.12}$$

Going from the first to the second line, we note that the rotation matrices in different sectors do not commute, hence the introduction of parameters $\tilde{f}$ and $\tilde{g_e}$. The lepton rotation in the (2 3) sector is still $-\pi/4$ up to corrections of order λ^2; the (1 2) mixing angle is corrected by an term of order λ from the maximal LO result and a large angle in the (1 3) sector is generated. For the quarks, only the Cabibbo angle is generated and it is of order λ as required; the other two angles are generated at even higher orders. The bimaximal leading order and next-to-leading order results for leptons are graphically summarized in figure 4.4; for quarks, it is the same as in figure 4.2.

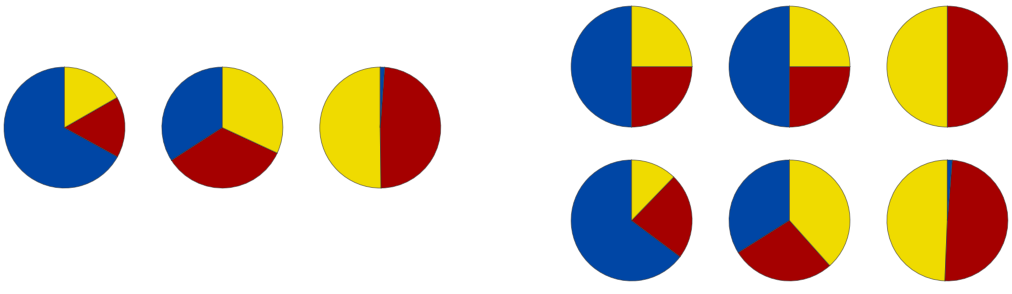

Figure 4.4: *Left: pie charts showing the flavour content of the three neutrino eigenstates. Right: The bimaximal mixing pattern (upper line) and a possible NLO result if corrections of the size λ are allowed in the (1 2) and (1 3) but not the (2 3) sector as in the model of this chapter. We have used $\delta\theta^l_{12} = -0.7\theta_C$ and $\delta\theta^l_{13} = 0.5.\theta_C$*

We end this section with a continuation of the wishlist we ended the previous section with. With respect to mixing angles in the lepton and quark sectors, the model should have the following properties.

- Show bimaximal lepton mixing and no quark mixing at leading order.
- At next-to-leading order, have a correction of order λ to the (1 2) mixing angles of both leptons and quarks.
- The two other angles in the CKM matrix should be generated by higher order effects, such that $\theta^q_{23} \sim \lambda^2$ and $\theta^q_{13} \sim \lambda^3$.
- The atmospheric mixing angle θ^l_{23} may not get a NLO correction; its deviation from maximal is at most λ^2.
- The model should give a value or range for the reactor mixing angle θ^l_{13}. When the model was first constructed, $\theta^l_{13} > 0$ was only hinted at and the result $\theta^l_{13} = \mathcal{O}(\lambda)$ was a prediction – one that is indeed supported by the current stream of data.

We have already seen that if the neutrino and charged fermion mass matrices at NLO are given by respectively (4.9) and (4.10) all wishes can be realized, so basically the wishlist collapses to the realization of these two matrices.

4.4 The Grand Unified Theory of Pati and Salam

In section 1.3.3 we introduced grand unified theories (GUTs). The main motivation was the observation that the three gauge couplings of an supersymmetric extension of the Standard Model go through one point when plotted against energy. From this scale on, there might not be three separate gauge forces, but one GUT-force instead. From a theoretical point of view, the main gain is that the description of the gauge sector is thus much simpler.

Also in the elementary fermion sector, grand unified theories offer a much simpler picture. We recall from table 2.2 on page 21 that five or six representations are needed to describe the fermions of one family of the Standard Model, depending on the question whether the righthanded neutrino is taken into account or not. In this chapter we assume it exists. Six representations is already a relatively low number. The lefthanded lepton doublet contains two states, one that below the electroweak phase transition becomes an electron and one that becomes a neutrino. The states of the righthanded up and down quarks (or, equivalently, anti-up or anti-down quarks) both describe three colour states. The lefthanded quark doublet even contains six states: three colours of up and three of down quarks. These states are depicted in figure 4.5.

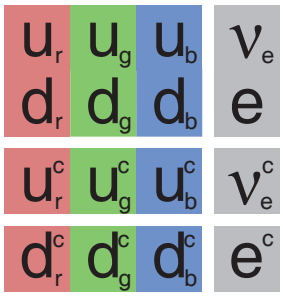

Figure 4.5: *The sixteen fermion states of the Standard Model grouped in six representations*

The way in which the fermions are grouped in figure 4.5 immediately suggests two possible unifications. Firstly, the difference between left- and righthanded fields are striking. While lefthanded fields are in a doublet, righthanded fields are in two separate singlets. The hypercharge is exactly such that these may be the two components of an $SU(2)_R$-doublet. This righthanded $SU(2)$ should then be present at high energies, but broken above the Standard Model scale. The assumption of this left-right symmetry closes the second horizontal gap in figure 4.5, thereby making it much more symmetric and compact.

Secondly, the position of the leptons right next to the quarks makes it tempting to see the leptons as a fourth colour. This is indeed possible if the $SU(3)$ gauge group of QCD is extended to $SU(4)$ at higher energies. As a result, the vertical gap in figure 4.5 is closed as well and all sixteen Standard Model states are described in just two representations, one lefthanded and one righthanded. We refer to these as F_L and F^c respectively. The fact that the theory is now completely left-right symmetric ensures anomaly cancellation.

The fact that quarks and leptons are treated on equal footing at high energies, with the symmetry broken in a very specific way, allows the bottom-tau unification and the mass relation (4.2) between muons and strange quarks. It is also essential in the generation of the mixing matrices from combined effects in both sectors.

The gauge group described above is known as the Pati–Salam grand unified theory [101]. Technically, it does not give a unified description. Even at high energies, the gauge group is the product of three groups and not a single group as is the case in the more conventional GUTs such as $SU(5)$ or $SO(10)$. Still, due to the unification of quarks and leptons and the fact that lefthanded and righthanded fields are treated on the same footing, we refer to it as a GUT.

The Pati–Salam Gauge group $SU(4)_{C'} \times SU(2)_L \times SU(2)_R$ is broken down to the Standard Model in two steps. At a very high scale M_C, the group $SU(4)_{C'}$ of extended colour breaks down to QCD $SU(3)_C$ times an additional $U(1)_{B-L}$. The charges of the known particles under this force are exactly the differences between their baryon and lepton number. At an intermediate scale M_R, $SU(2)_R \times U(1)_{B-L}$ is broken to $U(1)_Y$, the hypercharge of the Standard Model, according to $Y = T_{3R} + (B - L)/2$. The Standard Model gauge group now exists until the scale of electroweak symmetry breaking,

where the symmetry breaking ends at $SU(3)_C \times U(1)_{\rm em}$:

$$\begin{aligned} & SU(4)_{C'} \times SU(2)_L \times SU(2)_R \\ \xrightarrow{M_C} & SU(3)_C \times SU(2)_L \times SU(2)_R \times U(1)_{B-L} \\ \xrightarrow{M_R} & SU(3)_C \times SU(2)_L \times U(1)_Y \\ \xrightarrow{M_{\rm ew}} & SU(3)_C \times U(1)_{\rm em} \end{aligned} \tag{4.13}$$

We stress that the Pati–Salam GUT is not the only GUT that unifies many fermions in a single representation. In the $SU(5)$ GUT of Georgi and Glashow [102], the righthanded down quarks and the lepton doublet exactly have the right quantum numbers of the $\bar{5}$ of $SU(5)$, while the righthanded up quarks, the quark doublet and the righthanded electron together just fit in the anti-symmetric tensor representation 10. According to Georgi and Glashow, the arguments of unification are so strong that they are led "inescapably to the conclusion that $SU(5)$ is the gauge group of the world." In the $SO(10)$ GUT, the unification is even stronger as all 15 Standard Model particles plus the righthanded neutrino fit in the single 16 representation.

The choice for the Pati–Salam GUT over $SU(5)$ relates to the quark-lepton complementarity relations. In minimal $SU(5)$, one does not have equal charged lepton and down-type quark mass matrices as in equation (4.5). Instead the relation is $M_e \sim M_d^T$ and as result, a correction of order λ to the solar angle does not correspond to the Cabibbo angle of the CKM matrix.

On the other hand a reason to prefer Pati–Salam over $SO(10)$ is related to the type-I and type-II seesaw mechanisms. In these two GUT contexts, we expect both left-handed (LH) and right-handed (RH) neutrino Majorana mass matrices to be present. As a result, the effective LH neutrino mass matrix (4.7) gets contributions from both the type-I and II seesaw. In general, and this happens also in our proposal, this interplay introduces two mass scales and a highly non-trivial flavour structure for the effective neutrino mass matrix. It is difficult to find a realistic description of the PMNS matrix. For this reason, a hierarchy between the two contributions is usually assumed. We can reproduce quark-lepton complementarity in our model, if the type-II seesaw is dominant.

This possibility has already been investigated in several flavour GUT models, for example in [90,103–105] in the context of the $SO(10)$ GUT. However in [106] it was proven that the type-II dominance is not a viable solution in such GUTs. In the Pati–Salam context, there is more freedom and the eventual dominance of one of the two contributions could be realized. In this chapter we study the gauge Higgs potential and we verify that a type-II dominance can be justified, even if it puts strong constraints on the model building realization.

4.5 The flavour model building

In section 3.3.2 we found that the bimaximal mixing pattern can be reproduced by the 24-element discrete group S_4. For the group theory of S_4, we refer to appendix 3.B. In this section, we use a basis of S_4 different than the one in chapter 3. Obviously, the physical results are independent of the representation used. The representation chosen here makes the origin of the mixing effects from the charged lepton or neutrino sector more apparent. The transformations from this basis to bases with diagonal S or T is given in the appendix.

The spontaneous symmetry breaking of S_4 is responsible for the flavour structure of the matrices in equations (4.7) and (4.8): S_4 is broken down to two distinct subgroups and it is the presence of this mismatch at the LO which allows to construct M^ν and M^x. More in detail, the different subgroups to which S_4 is broken down are the subgroups that preserve the vevs of the flavons. In order to determine these structures, it is necessary to identify the elements of the group which leave the vevs of the flavons invariant under their action. Doing so, we find that S_4 is broken down to $Z_2 \times Z_2$ in the neutrino sector, originated by the elements ST^2S and T^3ST of the classes $3\mathcal{C}_2$ and $6\mathcal{C}_2$ respectively.

In the charged fermion sector, we find that S_4 is broken down to a $Z_2 \times Z_2$ group, distinct to the one in the neutrino sector, generated by the two elements T^2 and ST^2ST^3 of the classes $3\mathcal{C}_2$ and $6\mathcal{C}_2$ respectively.

It was already mentioned in section 2.3.2 that next to the non-Abelian S_4 auxiliary Abelian symmetries are required for a complete model. The complete flavour group is

$$G_f = S_4 \times Z_4 \times U(1)_{FN} \times U(1)_R \,. \tag{4.14}$$

The other terms in G_f carry out specific roles: the Abelian Z_4 symmetry is required to avoid dangerous terms in the superpotential, it helps to keep the different sectors of the model, quarks from leptons and neutrinos from charged leptons, separated; it is also useful in the generation of the flavon vacuum alignment. The continuous Frogatt-Nielsen (FN) Abelian symmetry, $U(1)_{FN}$, is introduced to justify charged fermion mass hierarchies. As in section 2.3.1, the (righthanded fields of the) first and second generation are assigned non-zero FN-charge, albeit a lower one than the one in section 2.3.1. This relates to the fact that mass terms for the first and second family often already require multiple (ordinary) flavons. The continuous R-symmetry $U(1)_R$, was introduced in section 2.4. It simplifies the constructions of the scalar potential. We stress again that the supersymmetric context is of great utility in the discussion of the scalar potential and helps in the gauge coupling running, but a similar non-supersymmetric model can in principle be constructed as well. In this chapter we only deal with SM particles and therefore we use the same symbols for a supermultiplet and its even R-parity components.

4.5.1 The matter, Higgs and flavon content of the model

As discussed in section 4.4, all fermionic matter of the SM plus a righthanded neutrino is contained in two Pati–Salam multiplets. The lefthanded multiplet F_L contains the quark and the lepton doublets, while the righthanded multiplet F^c contains the righthanded up quark, down quark, charged lepton and neutrino

$$\begin{aligned} \mathbf{SU(3)_C \times SU(2)_L \times U(1)_Y} &\quad\to\quad \mathbf{PS} \\ (3,\,2,\,1/6)_Q + (1,\,2,\,-1)_L &\quad\to\quad (4,\,2,\,1) \\ (\overline{3},\,1,\,-2/3)_{u^c} + (\overline{3},\,1,\,1/3)_{d^c} + (1,\,1,\,1)_{e^c} + (1,\,1,\,0)_{\nu^c} &\quad\to\quad (\overline{4},\,1,\,2)\,. \end{aligned} \tag{4.15}$$

The three copies of the LH supermultiplet are combined in the three-dimensional representation 3_1 of S_4, while the three families of the RH supermultiplet are in one of the 1-dimensional representations, 1_2, 1_2 and 1_1 respectively. The fact that we can put different representations within one family in different representations of the family symmetry group is essential here. Note that this would not be possible in (minimal) $SO(10)$, where all Standard Model particles are in one sixteen dimensional representation. The first two families are also charged under $U(1)_{FN}$ by two units. This suppresses their masses with respect to the third family ones. Further suppression of the first family with respect to the second is due to their different Z_4 charges that necessitate multiple flavon insertions already.

All the properties of the matter fields are summarized in table 4.2 and the unifying aspects are stressed in figure 4.6. Instead of 18 matter representations, as in the Standard Model, our model just needs four.

Our model contains five flavon fields that develop vacuum expectation values: two S_4 triplets (φ and φ') that, because of their Z_4 charge, deal at LO only with the Dirac Yukawa couplings of quarks and leptons, and two fields, one singlet (σ) and one triplet (χ), that, by Z_4, deal at LO only with the Majorana masses of neutrinos. The fifth flavon is the Froggatt–Nielsen messenger, which we indicate with θ. Their properties are shown in table 4.3. Under the continuous R-symmetry, the matter superfields transform as $U(1)_R = 1$, while all the flavons are neutral. Additional $U(1)_R = 2$ driving flavons are introduced in section 4.8. These help the original flavons obtaining their vevs.

Fermion masses and mixings arise from the spontaneous breaking of the flavour symmetry by means

Matter	F_L	F_1^c	F_2^c	F_3^c
PS	$(4,2,1)$	$(\overline{4},1,2)$	$(\overline{4},1,2)$	$(\overline{4},1,2)$
S_4	3_1	1_2	1_2	1_1
$U(1)_{FN}$	0	2	2	0
Z_4	1	1	i	$-i$

Table 4.2: *Transformation properties of the matter fields. Note that the PS assignments should be read in agreement with* $SU(4)_C \times SU(2)_L \times SU(2)_R$.

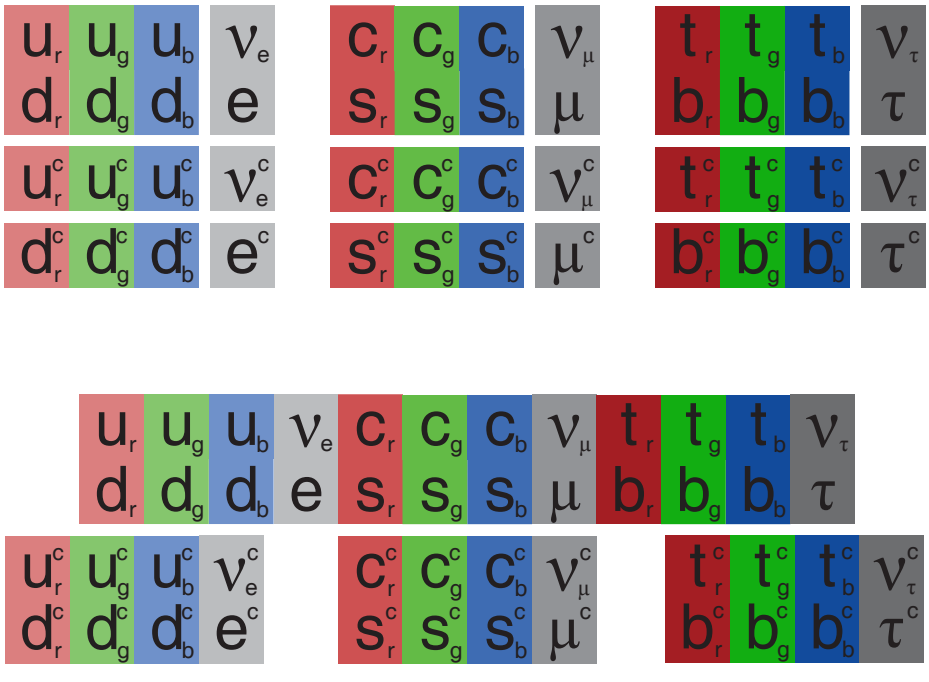

Figure 4.6: *The forty-eight fermion states of the Standard Model grouped in eighteen representations as in the SM (upper line) or in four representations as in our model (lower line)*

Flavons	θ	φ	φ'	χ	σ
S_4	1_1	3_1	3_2	3_1	1_1
$U(1)_{FN}$	-1	0	0	0	0
Z_4	1	i	i	1	1

Table 4.3: *The flavon field content and their transformation properties under the flavour symmetries. All flavon fields are singlet of the gauge group.*

of the flavons which develop vevs according to the following configuration: at LO we have

$$\langle\varphi\rangle = \begin{pmatrix} 0 \\ 1 \\ 1 \end{pmatrix} v_\varphi \ , \qquad \langle\varphi'\rangle = \begin{pmatrix} 0 \\ 1 \\ -1 \end{pmatrix} v_{\varphi'} \ , \tag{4.16}$$

$$\langle\chi\rangle = \begin{pmatrix} 0 \\ 0 \\ 1 \end{pmatrix} v_\chi \ , \qquad \langle\sigma\rangle = v_\sigma \ , \tag{4.17}$$

$$\langle\theta\rangle = v_\theta \ . \tag{4.18}$$

In this section we simply assume this vev alignment and we prove it to be a natural solution of the minimization of the scalar potential in section 4.8. Furthermore we assume that the FN messenger and the other flavons have vevs of the same order of magnitude: it results partly from the minimization procedure and partly from the constraints coming form the comparison with the measured mass hierarchies, as it will be clearer in the following.

The Higgs fields of our model relevant to build the fermion mass matrices transform under the gauge group and under the Z_4 factor of the flavour symmetry: in table 4.4 we summarize their transformation rules. The first three fields, ϕ, ϕ' and ρ, deal at LO only with the Dirac Yukawa couplings. Due to the Z_4 charges, ϕ and ϕ' are responsible for the third family and the charm quark masses, while ρ is responsible for the strange and μ masses. The field $\rho \sim (15, 2, 2)$ being in the adjoint of $SU(4)_C$ may develop vev along the $SU(4)_C$ direction diag$(-3, 1, 1, 1)$. This implies that the leptons which get mass via this field are a factor 3 heavier than the corresponding quarks and therefore this field is very useful to describe the second family, at least in the down sector, reproducing the well known Georgi–Jarlskog relation [99], $m_\mu \approx 3m_s$, at the high energy scale. As we show in the next sections, in order to recover the up-quark mass hierarchies the ρ projection along the light doublet Higgses, v^u_ρ and v^d_ρ, has to point only in the down direction: the requirement $v^u_\rho = 0$ can be realized only if the Higgs field content contains two identical copies of the Higgs field $(1, 2, 2)$ and this justifies the presence of both ϕ and ϕ'.

Finally, as we show in detail in the following sections, the field Δ_R is necessary to conclude the PS symmetry breaking pattern and to recover the SM gauge group through its spontaneous symmetry breaking vev. At the same time, when Δ_R develops a vev, it gives a Majorana mass to the right-handed neutrinos thus contributing to the effective neutrino mass matrix through the usual type-I seesaw mechanism. A second source for the neutrino mass matrix comes from Δ_L, in terms of the type-II seesaw mechanism.

Higgses	ϕ, ϕ'	ρ	Δ_L	Δ_R
PS	$(1, 2, 2)$	$(15, 2, 2)$	$(\overline{10}, 3, 1)$	$(10, 1, 3)$
Z_4	1	-1	1	-1

Table 4.4: *The Higgs fields responsible of generating fermion mass matrices and their transformation under the gauge and the Abelian flavour symmetries. All Higgs fields are singlets under $S_4 \times U(1)_{FN} \times U(1)_R$, while they can transform non-trivially under the Z_4 factor.*

In our scheme the neutrino mass matrix is dominated by type-II seesaw. As already stated in the two previous sections, the flavour structure of the effective neutrino mass matrix in equation (4.7) arises from an interplay between the two seesaw sources. In the PS context $m_D \sim M_u$ and this suggests a hierarchical structure for the type-I contribution, which does not agree with the flavour structure in (4.7). We show that, given $m_D \sim M_u$, the required flavour structure for the Majorana RH neutrino mass necessary to recover equation (4.7) is not allowed in our model. This suggests to find a construction in which the type-II contributions are dominating over the type-I and we show that such a feature puts strong constraints on the model building.

4.6 Fermion mass matrices at leading order

In this and the next section, we present the most important results: the fermion mass matrices and the resulting masses and mixings of the fermions. We first discuss the results at leading order in the flavon insertions. As expected for a model of bimaximal mixing, the results do not match the data very closely and next-to-leading order effects are very important as well. These are the topic of the next section.

The central object in the study of the fermion mass matrices is the matter superpotential, $\mathcal{W}_Y$. This Yukawa superpotential can be written as a sum of two pieces,

$$\mathcal{W}_Y = \mathcal{W}_{Dir} + \mathcal{W}_{Maj}. \tag{4.19}$$

These contain respectively terms with Dirac and Majorana structures. We study the superpotential making a power expansion in terms of flavon/Λ, distinguishing between leading and subleading couplings.

4.6.1 Dirac mass terms

We first study the Dirac matter superpotential at LO

$$\begin{aligned}\mathcal{W}^{LO}_{Dir} \;=\;& y_1 \frac{1}{\Lambda} F_L F^c_3 (\phi + \phi')\varphi + \\ &+ y_2 \frac{1}{\Lambda^3} F_L F^c_2 \theta^2 \rho \varphi' + \sum_{i=1}^{4} y_{3,(i)} \frac{1}{\Lambda^5} F_L F^c_2 \theta^2 (\phi + \phi') X^{(1)}_i + \\ &+ \sum_{i=1}^{3} y_{4,(i)} \frac{1}{\Lambda^4} F_L F^c_1 \theta^2 \rho X^{(2)}_i + y_5 \frac{1}{\Lambda^5} F_L F^c_1 \theta^2 (\phi + \phi') \chi^3 \,.\end{aligned} \tag{4.20}$$

Here we use a compact notation to avoid the proliferation of coefficients: the term $X^{(1,2)}_i$ represents a list of products defined as

$$\begin{aligned} X^{(1)}_i &\equiv \{\varphi^3,\, \varphi^2\varphi',\, \varphi\varphi'^2,\, \varphi'^3\}\,, \\ X^{(2)}_i &\equiv \{\varphi^2,\, \varphi\varphi',\, \varphi'^2\}\,. \end{aligned} \tag{4.21}$$

Each term represents all the different S_4 contractions which can be constructed with those flavons; furthermore we indicate with $y_1(\phi+\phi')$ the combination $y^{(1)}_1\phi + y^{(2)}_1\phi'$ and similarly for $y_{3,\,(i)}$ and y_5.

When the flavour symmetry is broken, the model describes a non-minimal PS model in which the Yukawa couplings present a well defined structure. Then, when the PS gauge symmetry is broken to the SM gauge group ϕ, ϕ' and the colour singlet component of ρ mix in four light Higgses, two up-type and two down-type, $h_{u,d}$ and $h'_{u,d}$. Thus at the EW scale ϕ, ϕ' and ρ have non-vanishing projections to the light Higgs components that acquire a vev. We indicate these components as $v^{u,d}_{\phi}$, $v^{u,d}_{\phi'}$ and $v^{u,d}_{\rho}$. As already said, we need to impose that the ρ field has no projection along the up direction: $v^u_\rho = 0$. This can be realized because in terms of the light Higgs up-vevs, $v^u_1 = \langle h_u \rangle$ and $v^u_2 = \langle h'_u \rangle$, v^u_ρ is given by

$$v^u_\rho = U_{13} v^u_1 + U_{23} v^u_2\,. \tag{4.22}$$

The matrix U is introduced in appendix 4.A. The constraint $v^u_2 = -U_{13}/U_{23} v^u_1$ can be imposed thanks to the freedom we have in the superpotential and in the soft potential[5]. Note that we could relax the condition $v^u_\rho = 0$ allowing a mild hierarchy between v^u_ρ and v^d_ρ, for example of order λ^2, without affecting the final mass hierarchies, but in the following, for simplicity, we work under the assumption that $v^u_\rho = 0$.

[5]This requirement, imposed *by hand*, could be motivated by some symmetry argument, but to introduce a mechanism that could explain $v^u_\rho = 0$, it would be necessary deeply modifying the structure of our model. In the present chapter we just assume this fine-tuning and we refer to the Appendix 4.A.2 for further details. We note that the fine-tuning we introduce in the model is similar to the fine-tuning which is universally accepted whenever the MSSM has to be recovered.

The final Dirac fermion mass matrices we get are given by

$$M_e^{LO} = -3\begin{pmatrix} 0 & 0 & 0 \\ 0 & y_2 & 0 \\ 0 & -y_2 & 0 \end{pmatrix} v_\rho^d \lambda^3 + \begin{pmatrix} 0 & 0 & 0 \\ 0 & 0 & y_1 \\ 0 & 0 & y_1 \end{pmatrix} v_\phi^d \lambda \,, \tag{4.23}$$

$$M_d^{LO} = \begin{pmatrix} 0 & 0 & 0 \\ 0 & y_2 & 0 \\ 0 & -y_2 & 0 \end{pmatrix} v_\rho^d \lambda^3 + \begin{pmatrix} 0 & 0 & 0 \\ 0 & 0 & y_1 \\ 0 & 0 & y_1 \end{pmatrix} v_\phi^d \lambda \,, \tag{4.24}$$

$$M_u^{LO} = m_D^{LO} = \begin{pmatrix} 0 & 0 & 0 \\ 0 & y_3 & 0 \\ 0 & -y_3 & 0 \end{pmatrix} v_\phi^u \lambda^5 + \begin{pmatrix} 0 & 0 & 0 \\ 0 & 0 & y_1 \\ 0 & 0 & y_1 \end{pmatrix} v_\phi^u \lambda \,. \tag{4.25}$$

We used the compact notation $y_i v_\phi^{u/d}$ to indicate $y_i^{(1)} v_\phi^{u/d} + y_i^{(2)} v_{\phi'}^{u/d}$ and absorbed all non-relevant CG coefficients. Note that y_3 is the sum of the different $y_{3,\,(i)}$ and that, by construction, $y_{1,2,3}$ can be considered complex coefficients with modulus of order 1. Note also that the different numerical coefficients between charged leptons and down quarks originate from to the presence of ρ instead of ϕ (ϕ') in the superpotential. The operators which should give contributions to the first families (those proportional to y_4 and y_5) are vanishing, thanks to the special flavon vev alignment. As a final comment, we are neglecting at this level of approximation the contributions to $M_{e,d}^{LO}$ coming from the operators proportional to y_3: these terms, which preserve the anti-alignment of the second and third entries of the second columns, are λ^2 suppressed with respect to the LO ones proportional to y_2.

The quark and lepton masses of the second and the third generation follow from (4.23)–(4.25)

$$\begin{aligned} m_\mu &\equiv -3\sqrt{2} y_2 v_\rho^d \lambda^3 \,, & m_\tau &\equiv \sqrt{2} y_1 v_\phi^d \lambda \,, \\ m_s &\equiv \sqrt{2} y_2 v_\rho^d \lambda^3 \,, & m_b &\equiv \sqrt{2} y_1 v_\phi^d \lambda \,, \\ m_c &\equiv \sqrt{2} y_3 v_\phi^u \lambda^5 \,, & m_t &\equiv \sqrt{2} y_1 v_\phi^u \lambda \,. \end{aligned} \tag{4.26}$$

We note that the top-quark Yukawa does not come from a renormalizable coupling; it has the same suppression as the other third family fermion masses. Obviously, the dominance of the top-quark mass should be justified by the hierarchy between v_ϕ^u and v_ϕ^d. The mass matrices in (4.23)–(4.25) are diagonalized by a maximal rotation in the sector (23), i.e. $U_e = V_d = V_u = R_{23}(\pi/4)$, while the fermion mass hierarchies are given by

$$\left|\frac{m_\mu}{m_\tau}\right| \sim \left|\frac{m_s}{m_b}\right| \sim \mathcal{O}(\lambda^2) \,, \qquad \left|\frac{m_c}{m_t}\right| \sim \mathcal{O}(\lambda^4) \,. \tag{4.27}$$

Furthermore, at the cut off, we recover some relations among the masses of different fermions: the $b - \tau$ unification and the Georgi–Jarlskog relation [99]

$$|m_\tau| = |m_b| \,, \qquad |m_\mu| = 3|m_s| \,. \tag{4.28}$$

Finally we should comment of the relative value of the top and of the bottom masses:

$$\left|\frac{m_t}{m_b}\right| = \left|\frac{y_1^{(1)} v_\phi^u + y_1^{(2)} v_{\phi'}^u}{y_1^{(1)} v_\phi^d + y_1^{(2)} v_{\phi'}^d}\right| \,. \tag{4.29}$$

Note that usually this ratio is proportional to $\tan\beta$, the ratio between the up- and down-vevs of the light Higgses, but this is not the case: indeed the light Higgses are combinations of ϕ, ϕ' and ρ and therefore we can define $\tan\beta$ as

$$\tan\beta \equiv \frac{\sqrt{(v_\phi^u)^2 + (v_{\phi'}^u)^2}}{\sqrt{(v_\phi^d)^2 + (v_{\phi'}^d)^2 + (v_\rho^d)^2}} \neq \left|\frac{m_t}{m_b}\right| \,. \tag{4.30}$$

4.6.2 Majorana mass terms

We now discuss the part of the superpotential which contains the Majorana couplings. At LO it is given by[6]

$$\mathcal{W}_{Maj}^{LO} = \tilde{k}_0\, F_L F_L \Delta_L + \sum_{i=1}^{2} \frac{\tilde{k}_{1,(i)}}{\Lambda}\, F_L F_L \Delta_L X_i^{(3)} + \sum_{i=1}^{3} \frac{\tilde{k}_{2,(i)}}{\Lambda^2} F_L F_L \Delta_L X_i^{(4)} + z_1\, F_3^c F_3^c \Delta_R \,. \tag{4.31}$$

This uses the compact notation

$$\begin{aligned} X^{(3)} &\equiv \{\chi,\, \sigma\}\,, \\ X^{(4)} &\equiv \{\chi^2,\, \chi\sigma,\, \sigma^2\}\,. \end{aligned} \tag{4.32}$$

This superpotential is responsible for giving the following Majorana LH and RH neutrino mass matrices:

$$M_L = \begin{pmatrix} k_0 & k_1\lambda & 0 \\ k_1\lambda & k_0 & 0 \\ 0 & 0 & k_0 + k_2\lambda^2 \end{pmatrix} v_L\,, \qquad M_R = \begin{pmatrix} 0 & 0 & 0 \\ 0 & 0 & 0 \\ 0 & 0 & z_1 \end{pmatrix} v_R\,. \tag{4.33}$$

Here v_L, v_R are the vevs of $\Delta_{L,R}$ respectively. At every order in λ, there is a diagonal contribution, parameterized by one of the $\tilde{k}_i$. The collective effect is captured in the effective parameter k_0 of order 1.

$$k_0 \equiv \tilde{k}_0 + \tilde{k}_{1,(2)}\lambda + \tilde{k}_{2,(1)}\lambda^2 + \tilde{k}_{2,(3)}\lambda^2 \tag{4.34}$$

In the same spirit we define k_1 and k_2

$$\begin{aligned} k_1 &\equiv \tilde{k}_{1,(1)} + \tilde{k}_{2,(2)}\lambda\,, \\ k_2 &\equiv -\tilde{k}_{2,(1)}\,. \end{aligned} \tag{4.35}$$

While M_L corresponds to the type-II contribution to the effective neutrino mass matrix, M_R provides a type-I term. Even at this approximation level, we note the tension between the two seesaw contributions: $m_\nu^{\text{(type-II)}} \equiv M_L$ presents a maximal rotation in the (12) sector, while it is easy to verify that $m_\nu^{\text{(type-I)}} \equiv m_D M_R^{-1} m_D^T$ shows a democratic structure on the (23) sector which corresponds to a maximal rotation here. To recover the mass matrix in (4.7) it is necessary that the type-II contribution dominates over the type-I terms: in this case it is sufficient to identify a with k_0, b with $k_1\lambda$ and c with $k_0 + k_2\lambda^2$.

The neutrino masses can be written as

$$|m_{1,2}|^2 = \Big(|k_0|^2 \mp 2|k_0|\,|k_1|\,\cos(\theta_{k_0} - \theta_{k_1})\lambda + |k_1|^2\,\lambda^2\Big) v_L^2\,, \tag{4.36}$$

$$|m_3|^2 = \Big(|k_0|^2 + 2|k_0|\,|k_2|\,\cos(\theta_{k_0} - \theta_{k_2})\lambda^2\Big) v_L^2\,. \tag{4.37}$$

Here θ_{k_i} is the argument of the complex number k_i. The definition of the solar mass difference implies that $|m_1|$ is smaller than $|m_2|$. This requires $\cos(\theta_{k_0} - \theta_{k_1}) > 0$. We see that in most of parameter space the spectrum is quasi degenerate, as the unsuppressed term with $|k_0|^2$ that appears in all three masses dominates over the other terms that are λ or λ^2 suppressed.

We also see that in most of the parameter space $|m_3|$ is the central eigenvalue: indeed $|m_1|$ ($|m_2|$) is shifted down (up) from the central value $|k_0|^2 v_L^2$ by a term proportional to λ, while $|m_3|$ stays closer to this central value as it is only shifted by a term proportional to λ^2. Having $|m_3|$ as the central eigenvalue is obviously in contradiction with experimental data. We conclude that our model is only viable when the term $2|k_0|\,|k_1|\,\cos(\theta_{k_0} - \theta_{k_1})\lambda$ is suppressed. This is clearly possible if either $|k_0|$ or $|k_1|$ or $\cos(\theta_{k_0} - \theta_{k_1})$ (or a combination of them) is small. In particular, the latter condition means that

[6] Regarding the terms which contribute to M_R, we consider at LO only the first non vanishing term in the superpotential.

k_0 and k_1 are almost perpendicular in the complex plane. We now investigate on these different scenarios, calculating the solar and atmospheric mass squared differences. Taking as definition of Δm^2_{atm} the mass squared difference between the heaviest and the lightest neutrinos, we have different results for normal (NO) and inverse (IO) mass ordering as given by

$$\begin{aligned}
\Delta m^2_{sol} &\equiv m_2^2 - m_1^2 \\
&= 4|k_0||k_1|\cos(\theta_{k_0}-\theta_{k_1})\lambda\, v_L^2\,, \\
\Delta m^2_{atm} &\equiv \begin{cases} \Delta m^2_{atmNO} \equiv (m_3^2 - m_1^2) \\ \Delta m^2_{atmIO} \equiv (m_2^2 - m_3^2) \end{cases} \\
&= \underbrace{2|k_0||k_1|\cos\left(\theta_{k_0}-\theta_{k_1}\right)\lambda\, v_L^2}_{\Delta m^2_{sol}/2} \mp\big(|k_1|^2 - 2|k_0||k_2|\cos\left(\theta_{k_0}-\theta_{k_2}\right)\big)\lambda^2\, v_L^2\,.
\end{aligned} \tag{4.38}$$

On the right-hand side of the last equation, the first term is suppressed by λ; the second one only by λ^2. We would be tempted to conclude that the first term gives the dominant contribution: it is however exactly this term that must be suppressed in order to avoid $|m_3|$ as the central eigenvalue. Furthermore, this term is equal to half of the solar mass squared difference that is about 30 times as small as the atmospheric splitting (see table 2.3). As a result, to recover a value for Δm^2_{atm} close to the measured one, we need that the second term on the right-hand side of equation (4.38) is the dominant one. We can estimate the ratio between the two terms by calculating r, the ratio of the two mass squared differences:

$$\begin{aligned}
(r_{NO,IO})^{-1} &\equiv \frac{\Delta m^2_{atmNO,IO}}{\Delta m^2_{sol}} \\
&= \frac{2|k_0||k_1|\cos\left(\theta_{k_0}-\theta_{k_1}\right)\lambda \mp \big(|k_1|^2 - 2|k_0||k_2|\cos\left(\theta_{k_0}-\theta_{k_2}\right)\big)\lambda^2}{4|k_0||k_1|\cos\left(\theta_{k_0}-\theta_{k_1}\right)\lambda} \\
&= \frac{1}{2} \mp \frac{|k_1|^2 - 2|k_0||k_2|\cos\left(\theta_{k_0}-\theta_{k_2}\right)}{4|k_0||k_1|\cos\left(\theta_{k_0}-\theta_{k_1}\right)}\lambda\,.
\end{aligned} \tag{4.39}$$

The natural range of this quantity r^{-1} would be something like $[0.3-0.7]$ (central value 0.5 and corrections of order λ). However, measurements give $r = 0.032^{+0.006}_{-0.005} \approx \lambda^2$, or in other words $1/r \sim 30 \sim \lambda^{-2}$. We conclude that

$$\frac{4|k_0||k_1|\cos\left(\theta_{k_0}-\theta_{k_1}\right)}{\big||k_1|^2 - 2|k_0||k_2|\cos\left(\theta_{k_0}-\theta_{k_2}\right)\big|} \approx \lambda^3\,. \tag{4.40}$$

The most natural explanation may be assuming that $\cos\left(\theta_{k_0}-\theta_{k_1}\right)$ is very small. In that case the absolute values of all parameters can still be of order one, which was part of the naturalness requirement of the model. Neutrinos present a quasi degenerate (QD) spectrum and both normal and inverse ordering are possible. The typical scale of neutrino masses v_L is given in this case by

$$v_L^2 = \frac{\Delta m^2_{atm}}{\lambda^2\big||k_1|^2 - 2|k_0||k_2|\cos\left(\theta_{k_0}-\theta_{k_2}\right)\big|} \approx (0.1\text{eV})^2\,. \tag{4.41}$$

Possible alternative solutions of equation 4.40 that give a non-QD spectrum can be obtained only by admitting the parameters belong to a larger and less natural, range, $\lambda^2 - \lambda^{-2}$. In this case when k_0 is of order λ^{-2} and $\cos\left(\theta_{k_0}-\theta_{k_1}\right) \sim \lambda$ while $k_{1,2}$ still of order one a inverse hierarchical (IH) spectrum can be obtained. Another possibility to get an IH spectrum is having k_0 and $\cos\left(\theta_{k_0}-\theta_{k_1}\right)$ of order one, $k_1 \sim \lambda^{-1}$ and $k_2 \sim \lambda^2$. Finally a normal hierarchical (NH) spectrum can be obtained only in the case in which $k_2 \sim \lambda^{-2}$, $\cos\left(\theta_{k_0}-\theta_{k_1}\right)$ and k_1 of order 1 and $k_0 \sim \lambda^2$.

At this moment, we conclude that the quasi-degenerate hierarchy (with either ordering) is the most natural outcome of our model, while normal and inverse hierarchy solutions are also possible, albeit with slightly unnatural values of the parameters. In section 4.10 we find that the renormalization flow dramatically changes these predictions.

4.6.3 Mixing matrices at Leading Order

As anticipated, the mixing pattern at leading order is the bimaximal pattern that does not describe the data very well. Only considering the NLO contributions, which we study in the next section, the model agrees with the measurements.

$$V = \mathbb{1} \ , \qquad U = R_{23}\left(-\frac{\pi}{4}\right) R_{12}\left(\frac{\pi}{4}\right) = \begin{pmatrix} 1/\sqrt{2} & -1/\sqrt{2} & 0 \\ 1/2 & 1/2 & -1/\sqrt{2} \\ 1/2 & 1/2 & +1/\sqrt{2} \end{pmatrix} \ . \tag{4.42}$$

4.7 Fermion mass matrices at higher orders

The NLO contributions in the mass matrices originate from two sources: the first are the higher order terms in the superpotential, while the others come from the insertion of the NLO flavon vevs in the operators in equations (4.20, 4.31). In section 4.8 we show how the flavons develop vevs and how they are corrected. Here we anticipate the results, reporting the flavon vevs in a form which is useful for the discussion in this section:

$$\begin{aligned} \langle\varphi\rangle &= \begin{pmatrix} 0 \\ 1 \\ 1 \end{pmatrix} v_\varphi + \begin{pmatrix} 1 \\ 0 \\ 0 \end{pmatrix} \delta v_\varphi \ , & \langle\varphi'\rangle &= \begin{pmatrix} 0 \\ 1 \\ -1 \end{pmatrix} v_{\varphi'} + \begin{pmatrix} 1 \\ 0 \\ 0 \end{pmatrix} \delta v_{\varphi'} \ , \\ \langle\chi\rangle &= \begin{pmatrix} 0 \\ 0 \\ 1 \end{pmatrix} v_\chi + \begin{pmatrix} 0 \\ 1 \\ 0 \end{pmatrix} \delta^2 v_\chi \ , & \langle\sigma\rangle &= v_\sigma \ . \end{aligned} \tag{4.43}$$

Some comments are in place: the subleading corrections are suppressed with respect the LO terms as $\delta v/v \sim \lambda$ and $\delta^2 v/v \sim \lambda^2$ for each flavon; NLO corrections to the second and third entries of $\langle\varphi\rangle$ and $\langle\varphi'\rangle$ are present, but they present the same structure of the LO terms and can be re-absorbed; similarly, the NLO corrections to the third entry of $\langle\chi\rangle$ and to $\langle\sigma\rangle$ are present, but they can be re-absorbed into the LO terms; the other entries of $\langle\chi\rangle$ do not receive any corrections at NLO. If we consider the NNLO approximation level, i.e. corrections of relative order λ^2 with respect the LO terms, we see that the second and the third entries of $\langle\varphi\rangle$ ($\langle\varphi'\rangle$) are not (anti-)aligned anymore and that the second entry of $\langle\chi\rangle$ is filled in. It is interesting that the first entry of $\langle\chi\rangle$ is still vanishing at this level. We will see the relevance of this structure in a while.

4.7.1 Dirac mass terms

The Dirac matter superpotential at NLO is given by

$$\begin{aligned} \mathcal{W}_{Dir}^{NLO} = & \sum_{i=1}^{3} y_{6,(i)} \frac{1}{\Lambda^2} F_L F_3^c (\phi + \phi') X_i^{(5)} + \\ & + \sum_{i=1}^{3} y_{7,(i)} \frac{1}{\Lambda^4} F_L F_2^c \theta^2 \rho X_i^{(6)} + \sum_{i=1}^{8} y_{8,(i)} \frac{1}{\Lambda^6} F_L F_2^c \theta^2 (\phi + \phi') X_i^{(7)} + \\ & + \sum_{i=1}^{6} y_{9,(i)} \frac{1}{\Lambda^5} F_L F_1^c \theta^2 \rho X_i^{(8)} + \sum_{i=1}^{7} y_{10,(i)} \frac{1}{\Lambda^6} F_L F_1^c \theta^2 (\phi + \phi') X_i^{(9)} + \\ & + \sum_{i=1}^{13} y_{11,(i)} \frac{1}{\Lambda^7} F_L F_1^c \theta^2 (\phi + \phi') X_i^{(10)} \ . \end{aligned} \tag{4.44}$$

We adopt a compact notation similar to the one in equation (4.20):

$$\begin{aligned}
X_i^{(5)} &\equiv \{\varphi\sigma,\, \varphi\chi,\, \varphi'\chi\}\,, \\
X_i^{(6)} &\equiv \{\varphi'\sigma,\, \varphi\chi,\, \varphi'\chi\}\,, \\
X_i^{(7)} &\equiv \{\varphi^3\chi,\, \varphi^2\varphi'\chi,\, \varphi\varphi'^2\chi,\, \varphi'^3\chi,\, \varphi^3\sigma,\, \varphi^2\varphi'\sigma,\, \varphi\varphi'^2\sigma,\, \varphi'^3\sigma\}\,, \\
X_i^{(8)} &\equiv \{\varphi^2\chi,\, \varphi\varphi'\chi,\, \varphi'^2\chi,\, \varphi^2\sigma,\, \varphi\varphi'\sigma,\, \varphi'^2\sigma\}\,, \\
X_i^{(9)} &\equiv \{\varphi^4,\, \varphi^3\varphi',\, \varphi^2\varphi'^2,\, \varphi\varphi'^3,\, \varphi'^4,\, \chi^4,\, \chi^3\sigma\}\,, \\
X_i^{(10)} &\equiv \{\varphi^4\chi,\, \varphi^3\varphi'\chi,\, \varphi^2\varphi'^2\chi,\, \varphi\varphi'^3\chi,\, \varphi'^4\chi,\, \varphi^4\sigma,\, \varphi^3\varphi'\sigma,\, \varphi^2\varphi'^2\sigma,\, \varphi\varphi'^3\sigma, \\
&\qquad \varphi'^4\sigma,\, \chi^5,\, \chi^4\sigma,\, \chi^3\sigma^2\}\,.
\end{aligned} \tag{4.45}$$

Note that not all of these terms are non-vanishing when the flavons develop a vev: in particular $X_i^{(9)}$ for any i do not give a contribution when the LO vevs are considered: only when the corrections to the vevs are introduced, they contribute to the mass matrices. For this reason also the terms with $X_i^{(10)}$ are taken into account, even if they are suppressed by an additional Λ. The other terms which are vanishing at this order of approximation are $X_i^{(8)}$ for $i = 4, 5, 6$ and $X_i^{(10)}$ for $i = 6, \ldots, 13$. When flavons and Higgs fields develop vevs, we get the following Dirac mass matrices:

$$M_e^{NLO} = -3 \begin{pmatrix} 0 & 0 & 0 \\ \tilde{y}_4 & 0 & 0 \\ \tilde{y}_9 & 0 & 0 \end{pmatrix} v_\rho^d \lambda^5 - 3 \begin{pmatrix} 0 & \tilde{y}_7\lambda & 0 \\ 0 & \tilde{y}_2 & 0 \\ 0 & -\tilde{y}_2 & 0 \end{pmatrix} v_\rho^d \lambda^3 + \begin{pmatrix} 0 & 0 & \tilde{y}_6\lambda \\ 0 & 0 & \tilde{y}_1 \\ 0 & 0 & \tilde{y}_1 \end{pmatrix} v_\phi^d \lambda\,, \tag{4.46}$$

$$M_d^{NLO} = \begin{pmatrix} 0 & 0 & 0 \\ \tilde{y}_4 & 0 & 0 \\ \tilde{y}_9 & 0 & 0 \end{pmatrix} v_\rho^d \lambda^5 + \begin{pmatrix} 0 & \tilde{y}_7\lambda & 0 \\ 0 & \tilde{y}_2 & 0 \\ 0 & -\tilde{y}_2 & 0 \end{pmatrix} v_\rho^d \lambda^3 + \begin{pmatrix} 0 & 0 & \tilde{y}_6\lambda \\ 0 & 0 & \tilde{y}_1 \\ 0 & 0 & \tilde{y}_1 \end{pmatrix} v_\phi^d \lambda\,, \tag{4.47}$$

$$M_u^{NLO} = \begin{pmatrix} 0 & 0 & 0 \\ \tilde{y}_5 & 0 & 0 \\ \tilde{y}_{10} & 0 & 0 \end{pmatrix} v_\phi^u \lambda^7 + \begin{pmatrix} 0 & \tilde{y}_8\lambda & 0 \\ 0 & \tilde{y}_3 & 0 \\ 0 & -\tilde{y}_3 & 0 \end{pmatrix} v_\phi^u \lambda^5 + \begin{pmatrix} 0 & 0 & \tilde{y}_6\lambda \\ 0 & 0 & \tilde{y}_1 \\ 0 & 0 & \tilde{y}_1 \end{pmatrix} v_\phi^u \lambda\,. \tag{4.48}$$

At this order, the neutrino Dirac matrix still equals the up-type quark matrix $m_D^{NLO} = M_u^{NLO}$. In the above equations we used the definitions

$$\begin{aligned}
\tilde{y}_1 &\equiv y_1 + y_{6,(1)}\lambda\,, \\
\tilde{y}_2 &\equiv y_2 + y_{7,(1)}\lambda\,, \\
\tilde{y}_3 &\equiv y_3 + \textstyle\sum_{i=5}^{8} y_{6,(i)}\lambda\,, \\
\tilde{y}_4 &\equiv \mathcal{F}_1[y_{9,(i)}] + \frac{1}{\lambda} y_4 \left(\frac{\delta v_{\varphi'}}{v_{\varphi'}} - \frac{\delta v_\varphi}{v_\varphi} \right)\,, \\
\tilde{y}_5 &\equiv \mathcal{F}_2\left[y_{11,(i)}\right] + \frac{1}{\lambda}\mathcal{F}_3\left[y_{10,(i)};\, \frac{\delta v_\varphi}{v_\varphi},\, \frac{\delta v_{\varphi'}}{v_{\varphi'}}\right] + \frac{1}{\lambda^2}\mathcal{F}_4\left[y_5;\, \frac{\delta^2 v_\chi}{v_\chi}\right]\,, \\
\tilde{y}_6 &\equiv (y_{6,(2)} + y_{6,(3)}) + \frac{1}{\lambda} y_1 \frac{\delta v_\varphi}{v_\varphi}\,, \\
\tilde{y}_7 &\equiv (y_{7,(2)} + y_{7,(3)}) + \frac{1}{\lambda} y_2 \frac{\delta v_{\varphi'}}{v_{\varphi'}}\,, \\
\tilde{y}_8 &\equiv \textstyle\sum_{i=1}^{4} y_{8,(i)} + \frac{1}{\lambda} \sum_{i=2}^{4} y_{3,(i)} \frac{\delta v_{\varphi'}}{v_{\varphi'}}\,, \\
\tilde{y}_9 &\equiv \mathcal{F}_5[y_{9,(i)}] + \frac{1}{\lambda} y_4 \left(\frac{\delta v_{\varphi'}}{v_{\varphi'}} + \frac{\delta v_\varphi}{v_\varphi} \right)\,, \\
\tilde{y}_{10} &\equiv \mathcal{F}_6\left[y_{11,(i)}\right] + \frac{1}{\lambda}\mathcal{F}_7\left[y_{10,(i)};\, \frac{\delta v_\varphi}{v_\varphi},\, \frac{\delta v_{\varphi'}}{v_{\varphi'}}\right]\,.
\end{aligned} \tag{4.49}$$

In the previous definitions we can see that each $\tilde{y}$ is the sum of two pieces: the first refers to the terms in equation (4.44) when the LO flavon vevs are considered; the second comes from the terms in equation (4.20) where the NLO flavon vevs are introduced. The only exception is $\mathcal{F}_3$ which refers to the term proportional to $X_i^{(9)}$ in equation (4.44) and that give contribution only when the NLO flavon vevs are considered. These two parts are of the same order of magnitude, since $\delta v/v \sim \lambda$ and $\delta^2 v/v \sim \lambda^2$. Note that $\mathcal{F}_i$ are distinct linear combinations of the arguments in the square brackets. The expressions in equations (4.46, 4.47, 4.48) are valid at NLO level. Note that the (anti-)alignment between the second and third entries of the (second) third families are still preserved. When considering higher order terms, this feature is lost and the $(1,1)$ entry of each mass matrix is filled.

The values for the charged fermion masses given in equation (4.26) are modified only by substituting the coefficients y_i with their tilde-versions:

$$y_1 \to \tilde{y}_1 \ , \qquad y_2 \to \tilde{y}_2 \ , \qquad y_3 \to \tilde{y}_3 \ . \tag{4.50}$$

At this approximation level, the first family masses are not yet well-described, because they are too small. We come back to these light masses in section 4.7.4.

4.7.2 Majorana mass terms

Moving to the Majorana part of the matter superpotential at NLO, we get

$$\begin{aligned}
\mathcal{W}_{Maj}^{NLO} \ = & \sum_{i=1}^{3} \frac{k_{3,(i)}}{\Lambda^3} F_L F_L \Delta_L X_i^{(11)} + \frac{z_2}{\Lambda^4} F_2^c F_2^c \theta^4 \Delta_R + \\
& + \frac{z_{3,(1)}}{\Lambda^4} F_2^c F_3^c \theta^2 \Delta_R \varphi\varphi' + \sum_{i=2}^{3} \frac{z_{3,(i)}}{\Lambda^5} F_2^c F_3^c \theta^2 \Delta_R X_{i-1}^{(12)} + \sum_{i=4}^{6} \frac{z_{3,(i)}}{\Lambda^6} F_2^c F_3^c \theta^2 \Delta_R X_{i-3}^{(13)} + \\
& + \sum_{i=1}^{4} \frac{z_{4,(i)}}{\Lambda^5} F_1^c F_3^c \theta^2 \Delta_R X_i^{(1)} + \sum_{i=5}^{12} \frac{z_{4,(i)}}{\Lambda^6} F_1^c F_3^c \theta^2 \Delta_R X_{i-4}^{(14)} + \\
& + \frac{z_5}{\Lambda^6} F_1^c F_2^c \theta^4 \Delta_R \varphi\chi + \sum_{i=1}^{2} \frac{z_{6,(i)}}{\Lambda^6} F_1^c F_1^c \theta^4 X_i^{(15)} \ .
\end{aligned} \tag{4.51}$$

As usual we used compact notation with

$$\begin{aligned}
X_i^{(11)} &\equiv \{\chi^3,\, \chi^2\sigma,\, \sigma^3\} \ , \\
X_i^{(12)} &\equiv \{\varphi\varphi'\chi,\, \varphi\varphi'\sigma\} \ , \\
X_i^{(13)} &\equiv \{\varphi^2\chi^2,\, \varphi\varphi'\chi^2,\, \varphi'^2\chi^2\} \ , \\
X_i^{(14)} &\equiv \{\varphi^3\chi,\, \varphi^2\varphi'\chi,\, \varphi\varphi'^2\chi,\, \varphi'^3\chi,\, \varphi^3\sigma,\, \varphi^2\varphi'\sigma,\, \varphi\varphi'^2\sigma,\, \varphi'^3\sigma\} \ , \\
X_i^{(15)} &\equiv \{\varphi^2,\, \varphi'^2\} \ .
\end{aligned} \tag{4.52}$$

A few comments are in place. Note that all the terms proportional to k_3 can be reabsorbed by a redefinition of $\tilde{k}_{0,1,2}$ and that the only new structure which corrects $\mathcal{M}_L$ comes from the term $F_L F_L \Delta_L \chi$ when we consider the subleading corrections of $\langle\chi\rangle$: as a result the entries $(1,3)$ and $(3,1)$ of $\mathcal{M}_L$ are filled in by terms proportional to λ^3. Regarding the contributions to the Majorana mass matrix for the RH neutrinos, it is important to see that the terms proportional to $z_{3,(i)}$ with $i = 1, \ldots, 3$ and to $z_{4,(i)}$ with $i = 1, \ldots, 4$ are vanishing, due to the particular flavon vev alignment of the model. As a consequence all the NLO contributions to $\mathcal{M}_R$ are of the order of λ^6, apart that one to the entry $(2,2)$ which is of the order of λ^4. Finally, we note that each entry of $\mathcal{M}_R$ is independent from all the others, being F_i^c singlets of the flavour symmetry, and therefore all the z_i are free parameters with

modulus of order 1. We listed only the dominant contributions, but the higher order terms would correspond to subleading corrections, which we can safely neglect in the following.

As a result of this analysis the Majorana masses for LH and RH neutrinos are given by

$$M_L^{NLO} = \begin{pmatrix} k'_0 & k'_1\lambda & k'_3\lambda^3 \\ k'_1\lambda & k'_0 & 0 \\ k'_3\lambda^3 & 0 & k'_0 + k'_2\lambda^2 \end{pmatrix} v_L \ , \qquad M_R^{NLO} = \begin{pmatrix} z_6\lambda^6 & z_5\lambda^6 & z_4\lambda^6 \\ z_5\lambda^6 & z_2\lambda^4 & z_3\lambda^6 \\ z_4\lambda^6 & z_3\lambda^6 & z_1 \end{pmatrix} v_R \ . \tag{4.53}$$

With the notation k'_i we account for all the redefinitions done on the parameters. As already stated when discussing the LO mass matrices, the contributions to the effective light-neutrino mass matrix come from the type-I and type-II seesaw mechanisms. The resulting NLO $m_\nu^{\text{(type-I)}}$ is given by

$$\begin{aligned} m_\nu^{\text{(type-I)}} &= m_D^{NLO}(M_R^{NLO})^{-1}(m_D^{NLO})^T \\ &= \begin{pmatrix} \tilde{y}_6^2\lambda^2 & \tilde{y}_1\tilde{y}_6\lambda & \tilde{y}_1\tilde{y}_6\lambda \\ \tilde{y}_1\tilde{y}_6\lambda & \tilde{y}_1^2 & \tilde{y}_1^2 \\ \tilde{y}_1\tilde{y}_6\lambda & \tilde{y}_1^2 & \tilde{y}_1^2 \end{pmatrix} \frac{(v_\phi^u)^2\lambda^2}{z_1 v_R} \ , \end{aligned} \tag{4.54}$$

This is diagonalized by a maximal rotation in the $(2\ 3)$ sector and not in the $(1\ 2)$ sector as demanded by equation 4.6. As a result, we need that the type-I seesaw contribution suppressed with respect to type-II seesaw one by at least a factor of order λ^2. Using equation (4.50), this translates to

$$\frac{m_t^2}{z_1 v_R} \leq \lambda^2 k'_0 v_L \ . \tag{4.55}$$

We remind here that v_L, v_R are the vevs of Δ_L and Δ_R respectively. In particular v_L is the vev developed by the SM $(1,3,1)$ triplet component of Δ_L and it is induced once the EW symmetry is broken. As we show in detail in the next sections the physical SM triplet $T \sim (1,3,1)$ arises by the mixing between the SM $(1,3,1)$ components of Δ_L and of two additional fields, Σ and Σ' transforming under the PS gauge symmetry as (1,3,3). The vev $\langle T \rangle$ of the $SU(2)_L$ triplet T is related to its mass M_T through the following expression

$$\langle T \rangle \simeq \alpha_{ij} \frac{v_i^u v_j^u}{M_T} \ . \tag{4.56}$$

Here α_{ij} are numerical coefficients arising by the details of the scalar potential and $v_1^u = \langle h_u \rangle \, , v_2^u = \langle h'_u \rangle$ are the vevs of the two up-type light Higgs doublets needed for the realization of our model (see appendix 4.A for details). Since v_L is the projection of $\langle T \rangle$ along Δ_L, neglecting fine tuned cases it is expected that

$$v_L \sim \langle T \rangle \ . \tag{4.57}$$

From equation (4.55) we need therefore that M_T and v_R satisfy

$$M_T \leq \lambda^2 \left(\frac{k'_0 z_1 \alpha_{ij} v_i^u v_j^u}{m_t^2} \right) v_R \, . \tag{4.58}$$

At the same time neutrino mass data imply that

$$k'_0 \alpha_{ij} \frac{v_i^u v_j^u}{M_T} \leq \mathcal{O}(1) \text{ eV} \, . \tag{4.59}$$

Combining the constraints of (4.58)–(4.59) we see that in the most natural scenario, assuming $\alpha_{ij} = 1$, M_T and v_R satisfy

$$\begin{gathered} v_R \gtrsim 30 \, M_T \ , \\ 10^{12} \, \text{GeV} \lesssim M_T \lesssim 10^{13} \, \text{GeV} \ . \end{gathered} \tag{4.60}$$

Nevertheless if we allow the numerical factors α_{ij} laying in the range $0.1 - 10$, then M_T, and consequently v_R, can be reduced even of two and one orders of magnitude respectively

$$10^{10} \, \text{GeV} \lesssim M_T \lesssim 10^{12} \, \text{GeV} \ . \tag{4.61}$$

In the following discussion of lepton mixing and in the phenomenological analysis, we assume that indeed type-II seesaw is dominating and neglect the type-I contributions. In the section devoted to the study of the scalar potential we justify this assumption and find the region of the parameters space where the type-II seesaw indeed dominates over type-I.

4.7.3 Mixing angles at the Next-to-Leading Order

Looking at equations (4.46)–(4.48) and (4.53) we see that the fermion mass matrices are of the required form as in (4.9) and (4.10). The resulting mixing matrices are modified with respect to the LO approximation and interesting new features follow. In the quark sector, the CKM matrix receives deviations from unity and at NLO the angle θ_{12}^q is not vanishing anymore:

$$\theta_{12}^q = \frac{\lambda}{\sqrt{2}} \frac{|\tilde{y}_7\tilde{y}_3 - \tilde{y}_2\tilde{y}_8|}{|\tilde{y}_2|\,|\tilde{y}_3|} \,. \tag{4.62}$$

Looking at this result, the meaning of the parameter λ is clear: it is defined as the ratio of the flavon vevs over the cut-off of the theory, but it also determines the order of magnitude of the Cabibbo angle. This justifies our initial assumption that λ is equal to 0.2. If the second columns of the up- and down-quark matrices are not proportional to each other, we can generate a non-vanishing Cabibbo angle θ_{12}^q, while the two other angles in the CKM matrix are still vanishing.

In the lepton sector, the PMNS is of the bimaximal form with large corrections as discussed in section 4.3. The solar and reactor angles are given by

$$\theta_{13}^l = \frac{\lambda}{2}\left|\frac{\tilde{y}_6}{\tilde{y}_1} - \frac{\tilde{y}_7}{\tilde{y}_2}\right|, \tag{4.63}$$

$$\theta_{12}^l = \frac{\pi}{4} - \frac{\lambda}{2}\left|\frac{\tilde{y}_6}{\tilde{y}_1} + \frac{\tilde{y}_7}{\tilde{y}_2}\right|. \tag{4.64}$$

As it is easy to see, the reactor angle and the deviation from the maximal value of the solar angle are of order λ and therefore the model is now in agreement with the experimental data[7], fulfilling the weak, but not the strong complementarity relations (4.4). At this approximation level, the atmospheric angle remains maximal. The relatively large value of θ_{13}^l was a prediction when this model was first presented.

4.7.4 Higher order effects

At the next-to-next-to-leading order (NNLO) and even higher orders, many new terms appear in the superpotential. However, only a few of them lead to new terms in the mass matrices, while the rest can be absorbed in redefinitions of the parameters as in equation (4.49). For this reason we do not report the full list of NNLO contributions, but we just comment on the physical consequences. Three effects are worth mentioning.

- As expected, the masses of the first families are strongly suppressed. We find that the down quarks and the electron masses are suppressed by a factor of λ^6 and the up-quark mass by a factor of λ^8. This leads to the following mass hierarchies in accordance with the wishlist of section 4.2
$$\left|\frac{m_d}{m_b}\right| \sim \left|\frac{m_e}{m_\tau}\right| \sim \lambda^5 \,, \qquad\qquad \left|\frac{m_u}{m_t}\right| \sim \lambda^7 \,. \tag{4.65}$$
- The (anti-)alignment of the (23) and (33) elements of the Dirac mass matrices in (4.46–4.48) gets broken as the new terms appear. The new elements are λ^2 suppressed with respect to the older

[7]Deriving equation (4.64), we already neglect the corrections which increase the value of the solar angle, instead of decreasing it

terms. As a result, the matrix that diagonalizes $M_i\, M_i^\dagger$, with $i = e, u, d$, has no longer an exact maximal mixing in the (2 3) sector. In the lepton sector, this translates to a λ^2 deviation from maximality in the atmospheric angle of the PMNS matrix. In the quark sector, the angle θ_{23}^q becomes of order λ^2. It is interesting to note that θ_{13}^q remains vanishing at this order. It only appears when even stronger suppressed terms are taken into account and is of order λ^3, in accordance with the Wolfenstein parametrization [21].

- The third columns of the mass matrices in (4.46)–(4.47) are proportional to v_ϕ^d, while the second column of M_d^{NLO} is proportional to v_ρ^d and that one of M_e^{NLO} to $-3v_\rho^d$. Therefore, also at NLO, equations (4.28) are fulfilled. At the NNLO level, terms proportional to v_ρ^d appear in the third columns of charged lepton and down-type quark matrices and terms proportional to v_ϕ^d in the second columns. The new terms are $\lambda^2 \approx 5\%$ suppressed with respect to the old entries. We thus expect deviations from the relations $|m_\tau| = |m_b|$ and $|m_\mu| = 3|m_s|$ at the 5% level.

After giving the right masses to the first generation fermions and introducing the (2 3) and (1 3) mixing angles in the CKM matrix, all points at the wishlists at the end of sections 4.2 and 4.3 are satisfied. So far, the model is successful. However, its success is based on a number of assumptions: that the flavons can indeed have the vacuum expectation value structure mentioned; that the Higgs fields indeed break the symmetry in the way assumed and that the values of fermion parameters derived at the high energy scale are still useful to describe physics when they are measured at low energy scales. These assumptions are studied in more detail in the next few sections.

4.8 The flavon scalar potential

In this section we comment on the vacuum alignment mechanism which explains the flavon vevs as in equations (4.16)–(4.18). It turns out that our desired alignment is exactly the one presented in [64], once we transform all the fields in our basis. Note indeed that it is possible to identify each flavon of table 4.3 with the flavons in [64], by simply comparing the transformation properties under the full flavour group:

$$\varphi \longrightarrow \varphi_l\ , \qquad \varphi' \longrightarrow \chi_l\ , \qquad \chi \longrightarrow \varphi_\nu\ , \qquad \sigma \longrightarrow \xi_\nu\ . \tag{4.66}$$

We use the unitary matrix Ω_T of appendix 3.B to move from the basis in [64] to our basis,

$$\begin{pmatrix} 1 & 0 & 0 \\ 0 & -i/\sqrt{2} & i/\sqrt{2} \\ 0 & 1/\sqrt{2} & 1/\sqrt{2} \end{pmatrix}\ . \tag{4.67}$$

We find (up to irrelevant phases) the following flavon vev alignment[8]. We comment about the presence of equivalent solutions below.

$$\varphi \propto \begin{pmatrix} 0 \\ 1 \\ 1 \end{pmatrix}\ , \qquad \varphi' \propto \begin{pmatrix} 0 \\ 1 \\ -1 \end{pmatrix}\ , \qquad \chi \propto \begin{pmatrix} 0 \\ 0 \\ 1 \end{pmatrix}\ . \tag{4.68}$$

These vacuum alignments correspond to equations (4.16)–(4.17).

The correct flavon vacuum alignment is ensured by a set of driving superfields among the same lines as described in section 2.4 dealing with a context similar to our model. All the driving fields transform as $U(1)_R = 2$ under the continuous R-symmetry and they appear linearly in the superpotential. In table 4.8 we show the driving fields and their transformation properties under $S_4 \times Z_4$.

It is easy to determine the correspondence between our set of driving fields and those of [64]:

$$D_R \longrightarrow \varphi_l^0\ , \qquad \varphi_R \longrightarrow \chi_l^0\ , \qquad \chi_R \longrightarrow \varphi_\nu^0\ , \qquad \sigma_R \longrightarrow \xi_\nu^0\ . \tag{4.69}$$

[8] The vevs of the fields φ and φ' is recovered by applying the unitary matrix in equation (4.67) to an equivalent configuration of equation (51) in [64], resulting from the application of the element $(TS)^2$ to (51) and of the element T to (18) of [64]

Driving	D_R	φ_R	χ_R	σ_R
S_4	2	3_2	3_1	1_1
Z_4	-1	-1	1	1

Table 4.5: *The driving field content and their transformation properties under $S_4 \times Z_4$. They are all singlets under the gauge group and the FN symmetry, while they transform as $U(1)_R = 2$ under the continuous R-symmetry.*

We now construct the driving superpotential w_d, which contains only flavons and driving fields and in particular neither matter fields nor Higgses, and look for the conditions that minimize the scalar potential,

$$V = \sum_i \left| \frac{\partial w_d}{\partial \Phi_i} \right|^2 + m_i^2 |\Phi_i|^2 + \dots \tag{4.70}$$

We write Φ_i to collectively denote all the scalar fields of the theory; m_i^2 are soft masses and dots stand for D-terms for the fields charged under gauge group and possible additional soft breaking terms. Since m_i^2 are expected to be much smaller that the mass scales involved in w_d, it is reasonable to minimize V in the supersymmetric limit and to account for soft breaking effects subsequently.

Since our flavon and driving field content exactly corresponds to the one in [64], we already know that the vev alignment in (4.16)–(4.17) represents an isolated minimum of the scalar potential. We only need to identify the relations which link the vevs v_φ, $v_{\varphi'}$, v_χ and v_σ among each other in our model. We therefore study the potential that can be constructed from the flavon driving fields and the ordinary flavons

$$\begin{aligned} w_d \; &= f_1 D_R \varphi\varphi + f_2 D_R \varphi'\varphi' + f_3 D_R \varphi\varphi' + f_4 \varphi_R \varphi\varphi' + \\ &+ M_1 \Lambda \chi_R \chi + f_5 \chi_R \chi\sigma + f_6 \chi_R \chi\chi + \\ &+ M_2^2 \Lambda^2 \sigma_R + M_3 \Lambda \sigma_R \sigma + f_7 \sigma_R \sigma\sigma + f_8 \sigma_R \chi\chi \; , \end{aligned} \tag{4.71}$$

The first line deals with only the fields φ and φ' and the other two with χ and σ. As also explained in [64], this leads to the alignment in equations (4.16, 4.17) where the vevs satisfy

$$\begin{gathered} f_1 v_\varphi^2 + f_2 v_{\varphi'}^2 + \sqrt{3} f_3 v_\varphi v_{\varphi'} = 0 \; , \\ v_\sigma = -\frac{M_1}{f_5} \; , \qquad\qquad v_\chi^2 = \frac{f_5^2 M_2^2 - f_5 M_1 M_3 + f_7 M_1^2}{2 f_5^2 f_8} \; . \end{gathered} \tag{4.72}$$

The solution in equations (4.16, 4.17, 4.72) is not unique, but it is possible to introduce a set of soft supersymmetric breaking parameters, which selects this solution as the lowest minimum of the scalar potential.

It is interesting to note the presence of an other source of uncertainty in our solution, which minimizes V. Given the symmetry of w_d and the field configurations of (4.16, 4.17, 4.72), by acting on them with elements of the flavour symmetry group $S_4 \times Z_4$, we can generate other minima of the scalar potential. These alternative solutions however are physically equivalent to those of the original set and it is not restrictive to analyze the model by choosing as local minimum that one in equations (4.16, 4.17, 4.72).

The Froggatt–Nielsen field can acquire a vev through a D-term as given in equation (2.70)

$$|v_\theta|^2 = |\langle\theta\rangle|^2 = \frac{M_{FI}^2}{g_{FN}} \; . \tag{4.73}$$

It is relevant to underline that the vevs in (4.72, 4.73), depend on mass parameters: all these mass scales naturally have the same order of magnitude and as a result $v_X/\Lambda_f \sim \lambda$. The only exceptions are the vevs of φ and φ', which depend on a flat direction. In the model, we simply assume that their vevs have values of the same order as all the other flavon vevs.

4.8.1 Higher order contributions

In this section we briefly comment on the corrections which enter in the flavon vevs, once the higher order contributions are taken into account. We leave all details to appendix 4.B.

In the superpotential w_d, the flavons which contribute to the Dirac mass terms, φ and φ', and those which contribute to the Majorana mass terms, χ and σ, at LO belong to two separate sectors, indeed any mixing term is prevented due to the Z_4 symmetry. This situation is not preserved at NLO, since the fields χ and σ are neutral under the Z_4 symmetry and therefore we can add each of them to all the terms in w_d. This leads to modifications to the LO vev alignment of (4.16) and it turns out that the first entries of $\langle\varphi\rangle$ and $\langle\varphi'\rangle$ are filled in, while the second and third entries are corrected by terms which can be however absorbed into the LO ones, without spoiling the alignment. Also the vevs in equation (4.17) receive some corrections: the first and second entries of $\langle\chi\rangle$ still vanish and the NLO contributions to the third entry can again be absorbed into the LO term. This discussion justifies the results showed in equation (4.43).

Corrections from the NNLO contributions are without particular alignments: in particular, the second and third entries of $\langle\varphi\rangle$ and $\langle\varphi'\rangle$ are no longer related, and also the second entry of $\langle\chi\rangle$ gets a non-zero value. It is interesting to note that the first entry of $\langle\chi\rangle$ remains zero.

4.9 Higgs scalar potential

In this section we present the study of the Higgs potential in our model. It is an interesting example of how the introduction of flavour symmetries and the assumptions made to get the correct mass matrices have non-negligible consequences on the Higgs sector. As a result, the study of the Higgs scalar potential and of the gauge and the running Yukawa couplings in a general non-flavour PS context does not strictly hold. Note that even if the following analysis refers to our particular choice of fields and symmetries, our conclusions can be taken as a general hint for a very large class of models that combine a discrete flavour symmetry with a grand unified scenario: indeed our model building strategy shares common features with other constructions. In particular the Higgs fields usually transform under the flavour symmetry G_f – in our case under the Z_4 part of it. This has direct consequences on the implementation of the grand unified symmetry breaking. Moreover type-II seesaw dominance and particular patterns of vanishing projections of the heavy Higgs fields on the light Higgs doublets are frequently required to get the correct fermion mass matrices.

In table 4.6 we list all the Higgs fields which are necessary to reproduce the correct mass matrices and to implement the desired PS symmetry breaking pattern. This extends table 4.4 that only contains that appear in the Yukawa superpotentials. The fields in table 4.6 carry one of the labels 'min' (from 'minimal'), 'ext' (from 'extended') or 'new'. This refers to the question whether they occur already in minimal Pati–Salam scenarios, only in extended (non-minimal) realizations or are new to our construction that combines GUT with flavour.

Some of these Higgs fields are already present in the minimal version of PS models [107]: typically a (15,1,1) multiplet – as the fields A and B in table 4.6 – is used to break $SU(4)_C$ down to $SU(3)_C \times U(1)_{B-L}$ and to induce the vevs of the couple of $(10,1,3) \oplus (\overline{10},1,3)$ – corresponding to the fields $\Delta_R \oplus \overline{\Delta}_R$ in table 4.6. The latter vevs breaks $SU(2)_R \times U(1)_{B-L}$ into the SM hypercharge $U(1)_Y$ concluding the symmetry breaking chain from the PS gauge group to the SM $SU(3)_C \times SU(2)_L \times U(1)_Y$. The field that triggers the EW symmetry breaking is usually a bidoublet (1,2,2) – as ϕ or ϕ' in table 4.6. The fields $(\overline{10},3,1) \oplus (10,3,1)$ – the fields $\Delta_L \oplus \overline{\Delta}_L$ in table 4.6 – do not develop vevs at tree level in the usual minimal PS model, but only when next to leading order terms are taken into account; these are typically suppressed by the Planck scale, as already stated in [107]. For this reason in the minimal PS the type-II seesaw contributions to the effective neutrino masses are almost negligible.

We identify three main reasons for which the existent studies of the symmetry breaking patterns in

Higgses	ϕ	ϕ'	ρ	ξ	Δ_L	Δ_R
PS	$(1,2,2)$	$(1,2,2)$	$(15,2,2)$	$(1,1,1)$	$(\overline{10},3,1)$	$(10,1,3)$
Z_4	1	1	-1	-1	1	-1
	min	new	ext	new	ext	min
Higgses	$\overline{\Delta}_L$	$\overline{\Delta}_R$	A	B	Σ	Σ'
PS	$(10,3,1)$	$(\overline{10},1,3)$	$(15,1,1)$	$(15,1,1)$	$(1,3,3)$	$(1,3,3)$
Z_4	1	-1	1	-1	1	-1
	ext	min	min	new	ext	new

Table 4.6: *All the Higgs fields of the model and their transformation properties under the gauge group and under Z_4. All Higgs fields are invariant under the other factors of the flavour symmetry group G_f. The labels 'min', 'ext' and 'new' indicate whether the field is present in minimal PS models, in extended ones or only in our realization.*

the PS context have to be modified and this automatically justifies the presence of the new fields in table 4.6.

- The assumption $v_\rho^u = 0$ necessary to distinguish the up-quark sector from the others and to recover the up-quark mass hierarchies can be realized only if we include two identical copies of bidoublet (1,2,2), ϕ and ϕ' (see details in appendix 4.A), and we then impose that four $SU(2)_L$ doublets (2 up-type and 2 down-type) remain light;

- Since the fields ρ, Δ_R and $\overline{\Delta}_R$ transform non-trivially under the flavour symmetry Z_4, it is necessary to introduce two copies of (15,1,1) multiplets, A and B, with opposite Z_4 charges, 1 and -1 respectively: A is responsible of inducing the breaking of $SU(2)_R$ through its coupling with Δ_R and $\overline{\Delta}_R$; B allows the coupling of the bidoublets ϕ, ϕ' with the bidoublet ρ. In this way all of these three fields have a non-vanishing projection on the light Higgs $SU(2)_L$ doublets;

- The component of Δ_L which corresponds to the usual SM triplet (1,3,1) can develop a vev once the EW symmetry is broken only in the presence of a trilinear coupling with the $SU(2)_L$ Higgs doublets. This coupling cannot be constructed with only the Higgs fields $\Delta_L \oplus \overline{\Delta}_L$ and the field content given in table 4.6. For this reason we need an additional field that mediates this coupling and the simplest choice would be a bitriplet $\Sigma \sim (1,3,3)$ that can couple with the fields ϕ, ϕ' or ρ and at the same time can mix with Δ_L, when Δ_R develops vev at the $SU(2)_R$ breaking scale. However, once more, the presence of the Z_4 symmetry obliges the introduction of two distinct (1,3,3) Higgs fields, Σ and Σ', with opposite Z_4 charges, 1 and -1 respectively. In this way Σ can couple to the bidoublets ϕ, ϕ' or ρ, while Σ' can mix with Δ_L. Finally, we need a new ingredient that mixes Σ with Σ': a PS singlet ξ charged -1 under Z_4 can do the job.

The scalar part of the superpotential is then given by[9]

$$\begin{aligned}\mathcal{W} =& \frac{1}{2}M_\phi\,\phi\phi + \frac{1}{2}M_{\phi'}\,\phi'\phi' + M_{\phi\phi'}\,\phi\phi' + \frac{1}{2}M_\rho\,\rho\rho + M_{\Delta_L}\,\Delta_L\overline{\Delta}_L + \\ &+ M_{\Delta_R}\,\Delta_R\overline{\Delta}_R + \frac{1}{2}M_A\,AA + \frac{1}{2}M_B\,BB + \frac{1}{2}M_\Sigma\Sigma\Sigma + \frac{1}{2}M_{\Sigma'}\Sigma'\Sigma' + \frac{1}{2}M_\xi\xi\xi + \\ &+ \lambda_\xi\Sigma\Sigma'\xi + \lambda_{\xi AB}AB\xi + \lambda_{\phi\rho}\phi B\rho + \lambda_{\phi'\rho}\phi' B\rho + \frac{1}{3}\lambda_A AAA + \\ &+ \frac{1}{2}\lambda_B BBA + \lambda_L\Delta_L\overline{\Delta}_L A + \lambda_R\Delta_R\overline{\Delta}_R A + \\ &+ \frac{1}{2}\lambda_{\phi\Sigma}\phi\phi\Sigma + \frac{1}{2}\lambda_{\phi'\Sigma}\phi'\phi'\Sigma + \lambda_{\phi\phi\Sigma}\phi'\phi\Sigma + \frac{1}{2}\lambda_{\rho\Sigma}\rho\rho\Sigma + \\ &+ \lambda_{\Delta\Sigma'}\Delta_L\overline{\Delta}_R\Sigma' + \overline{\lambda}_{\Delta\Sigma'}\Delta_R\overline{\Delta}_L\Sigma' + \frac{1}{3}\lambda_\Sigma\Sigma\Sigma\Sigma + \frac{1}{2}\lambda_{\Sigma'}\Sigma'\Sigma'\Sigma\,.\end{aligned} \tag{4.74}$$

The vacuum configuration at the GUT breaking scale is given by[10]

$$\langle\Delta_R\rangle = \left\langle\overline{\Delta}_R\right\rangle = M_R\,, \qquad \langle A\rangle = M_{C_1}\,, \qquad \langle B\rangle = M_{C_2}\,, \qquad \langle\xi\rangle = V_\xi\,. \tag{4.75}$$

The vevs $\langle A\rangle$ and $\langle B\rangle$ break the $SU(4)_C$ to $SU(3)_C\times U(1)_{B-L}$, while $\langle\Delta_R\rangle$ and $\left\langle\overline{\Delta}_R\right\rangle$ break $SU(4)_C\times SU(2)_R$ into $SU(3)_C\times U(1)_Y$. Therefore, given our field content, the colour breaking scale, $M_C = \mathrm{Max}(M_{C_1}, M_{C_2})$, is never smaller than the $SU(2)_R$ breaking scale, M_R. We may expect that $(M_{C_1}\sim M_{C_2}) = M_C$ but in principle they could be different. Finally V_ξ is expected to be close to the flavour breaking scale, due to the ξ gauge singlet nature.

The F-derivative system obtained by the superpotential (4.74) reads

$$\begin{aligned}&M_{\Delta_R} + \frac{3}{\sqrt{2}}\lambda_R M_{C_1} = 0\,,\\ &M_B M_{C_2}\sqrt{2}\lambda_B M_{C_1}M_{C_2} + \lambda_{AB\xi}M_{C_1}V_\xi = 0\,,\\ &M_A M_{C_1} + \frac{1}{\sqrt{2}}\lambda_B M_{C_2}^2 - \frac{2}{\sqrt{3}}\lambda_R M_R^2 + \sqrt{2}\lambda_A M_{C_1}^2 + \lambda_{AB\xi}M_{C_2}V_\xi = 0\,,\\ &M_\xi V_\xi + \lambda_{AB\xi}M_{C_1}M_{C_2} = 0\,.\end{aligned} \tag{4.76}$$

By solving the previous equations, we can express the mass parameters that enter in the superpotential in term of the dimensionless parameters λ_i and the physical breaking scales. All details regarding the mass spectrum are reported in the appendix 4.A, but some comments are in place. As in the minimal supersymmetric PS [107] when the singlet component of A develops a vev, there is an accidental $SU(3)$ symmetry involving Δ_R and $\overline{\Delta}_R$. When the singlet components of these fields acquire a vev the accidental symmetry is broken to $SU(2)$ giving rise to 5 Goldstone Bosons (GBs). At the same time $SU(2)_R\times U(1)_{B-L}$ is broken down to $U(1)_Y$, eating 3 of the 5 GBs. Therefore 2 of them, namely δ^{++} and $\overline{\delta}^{++}$ are left massless, down to the SUSY soft breaking scale ~ 1 TeV. This is a well known prediction of SUSY PS theories, which can be tested at LHC [108–111]. On the other hand, contrary to the minimal case described in [107], due to the mixing between the Higgs fields A and B, no colour octet is lighter than M_R.

In order to assure type-II dominance and to get the correct PS symmetry breaking pattern, it is necessary that $M_T \le M_R \le M_C \le V_\xi$. In the next section we present the constraints on the parameters that can be derived from this special mass ordering. For the moment, we just assume this scheme. Below we give the spectrum of the states that become massive at scales between M_{susy} and V_ξ. We express the states with the quantum numbers they would have under the Standard Model gauge group.

[9] All the Higgs fields are neutral under the continuous $U(1)_R$. The scalar superpotential explicitly breaks it, while preserving the usual R-parity. The terms in equation (4.74) can be generated from a $U(1)_R$-conserving superpotential in which the breaking is mediated by additional fields, which are $U(1)_R = 2$ and develop non-vanishing vevs. For instance the mass term $M_\phi\,\phi\phi$ can originate from a trilinear term $X\,\phi\phi$, when $\langle X\rangle = M_\phi$. Similarly the trilinear coupling $\lambda_\xi\Sigma\Sigma'\xi$ could originate by the non-renormalizable term $X\,\Sigma\Sigma'\xi/\Lambda'$, when $\langle X\rangle/\Lambda' = \lambda_\xi$ and Λ' is the energy scale of the dynamics of the field X. In our model we simply assume the existence of the terms in equation (4.74) in the superpotential and allow for an explicit breaking of the $U(1)_R$ symmetry in this sector.

[10] We redefine $\langle\Delta_R\rangle = v_R$ as $\langle\Delta_R\rangle = M_R$ in order to adapt to the usual notation.

1. At V_ξ

   At this scale we have two heavy $SU(2)_L$ triplets given in section 4.A.3.

2. Between V_ξ and M_C In this range a number of fields become massive. These are

   - all the SM singlets given in section 4.A.1 except one, called ξ_0,
   - the colour triplets given in section 4.A.1,
   - the colour octets given in section 4.A.1,
   - the heavy doublets given in section 4.A.2,
   - the two heavy couples of $SU(2)_L$ triplets given in section 4.A.3.

3. At M_C

   At the scale where the extended colour group of the Pati–Salam theory breaks the colour scalars originating by $\Delta_R \oplus \overline{\Delta}_R$, ρ and $\Delta_L \oplus \overline{\Delta}_L$ become massive. These are

   - the $SU(2)_L$ singlets given in section 4.A.1,
   - the $SU(2)_L$ doublets given in section 4.A.2,
   - the $SU(2)_L$ triplets given in section 4.A.3.

4. At M_R

   At the scale where the righthanded $SU(2)$ is broken, the singlet ξ_0 becomes massive;

5. At M_T

   At the scale M_T of the type-II seesaw, the light couple of $SU(2)_L$ triplets given in section 4.A.3 obtains a mass.

6. At M_{susy}, the supersymmetry scale, next to the familiar sparticles, we find

   - the scalar singlets δ^{++} and $\overline{\delta}^{++}$ given in section 4.A.1 – these are well known low-energy remnants of models with Pati–Salam unification,
   - the $SU(2)_L$ light doublets given in section 4.A.2.

With the Higgs field content given in tables 4.4 and 4.6 and the scalar spectrum so far sketched we can calculate the running of the gauge couplings and see if the conditions given in (4.60) or those in (4.61) can be satisfied. Furthermore, in the study of this running (see appendix 4.C for details) from the M_{GUT} to the EW scale we have to impose the following constraints.

- We should recover the EW values for α_3, α_2 and α_1, related to the gauge couplings of the SM gauge group ;
- At $M_R \leq M_C$ the hypercharge $U(1)_Y$ is obtained by the $SU(2)_R \times U(1)_{B-L}$ breaking;
- We impose $\alpha_{B-L} = \alpha_C$ at M_C ;
- The 'GUT scale' is defined as the scale at which the largest $\alpha_i = 1$. In this way we are sure to be in a perturbative regime up to the GUT scale and thus we are allowed to adopt the one-loop renormalization group equations (RGEs).

Even using all these constraints we are left with two more free parameters, the value of the $SU(4)_C$ and $SU(2)_R$ breaking scales, i.e. M_C and M_R respectively.

We adopt two distinct approaches, that we indicate as the *more constraining* and the *less constraining* ones. In the first case we define M_C to be the scale at which the largest α_i is equal or smaller than $1/4\pi$. In this way all the gauge coupling g_i are smaller than 1 at M_C . In the second case we allow the largest α_i to correspond to a gauge coupling in the range $1 < g_i < 3$, so $1/4\pi < \alpha_R < 9/4\pi$. Then M_R should satisfies equation (4.60) or (4.61), but its exact value is not fixed yet.

A few general comments are in place. The non-minimal PS field content affects the running of the gauge couplings in a non-negligible way. In particular the presence of the charged singlets δ^{++} and $\overline{\delta}^{++}$ down to M_{susy} deeply modifies the $U(1)_Y$ and $SU(2)_R$ gauge coupling evolution. It turns out that the largest α_i above the M_R scale is always α_R. Therefore the two approaches we described can be formulated as follows:

- More constraining approach $\Longleftrightarrow \alpha_R < 1/4\pi$, at M_C
- Less constraining approach $\Longleftrightarrow 1/4\pi < \alpha_R < 9/4\pi$, at M_C .

4.9.1 More constraining approach

In this case there are no solutions neither for the ranges of values of M_T and M_R given in equation (4.60) nor for those in (4.61). Indeed we find that $M_R \leq 10^{12}$ GeV, as can be seen in fig. 4.7. In other words if we adopt this constraining approach to fix the value of M_C, the type-I and type-II seesaw scales require Yukawa parameters which are at least two orders of magnitude far from their natural values to reproduce the correct neutrino mass scale. This solution is not satisfactory: in this case the type-II seesaw dominance is obtained by increasing the Yukawa couplings in the right neutrino sector and at the same time reducing the coupling of the left-handed neutrinos with the scalar triplet. Even if this may be considered a solution, the challenge was to provide a justification of type-II seesaw dominance through the analysis of the Higgs scalar potential and not by tuning the Yukawa parameters. Moreover we introduced a FN Abelian symmetry to explain the small ($\leq 10^{-2}$) Yukawa parameters necessary in the charged fermion sector to reproduce the correct mass hierarchies. The presence of Yukawa parameters of this order in the purely left-handed neutrino sector makes the introduction of the FN symmetry questionable.

4.9.2 Less constraining approach

In this case there are solutions only for the second range of values of M_T and M_R given in equation (4.61). As can be seen in fig. 4.8, M_R can now reach the value of 10^{13} GeV. The three scales M_R, M_C and M_{GUT} are compressed in a narrow region around 10^{13} GeV and therefore our model is described by an extended MSSM model almost up to the GUT scale, defined as the scale where one of the couplings – in practice g_R – becomes non-perturbative [11], i.e. $\alpha_i > 1$. Nevertheless, the PS origin is reflected in the non-trivial relations between the Yukawa couplings. In conclusion, by admitting the Yukawa parameters span in a range 0.1–10. The scales M_R, M_C and M_{GUT} are driven to be very close to each other; we have found a narrow region of the parameter space where our model could still give a realistic description of fermion masses and mixings and in which type-II seesaw dominance is not imposed by hand.

To finally consider our model viable, we should study the stability of the flavour structure of the mass matrices under the RGEs from the GUT scale down to the EW one. The study of the full set of the

[11] Above this energy scale an other gauge structure could be active. We do not take in consideration an high-energy completion of the model, but it is reasonable that larger gauge groups or particular constructions could be present at these energies: for example an $SO(10)$ inspired approach in which fermions do not belong to a unique representation.

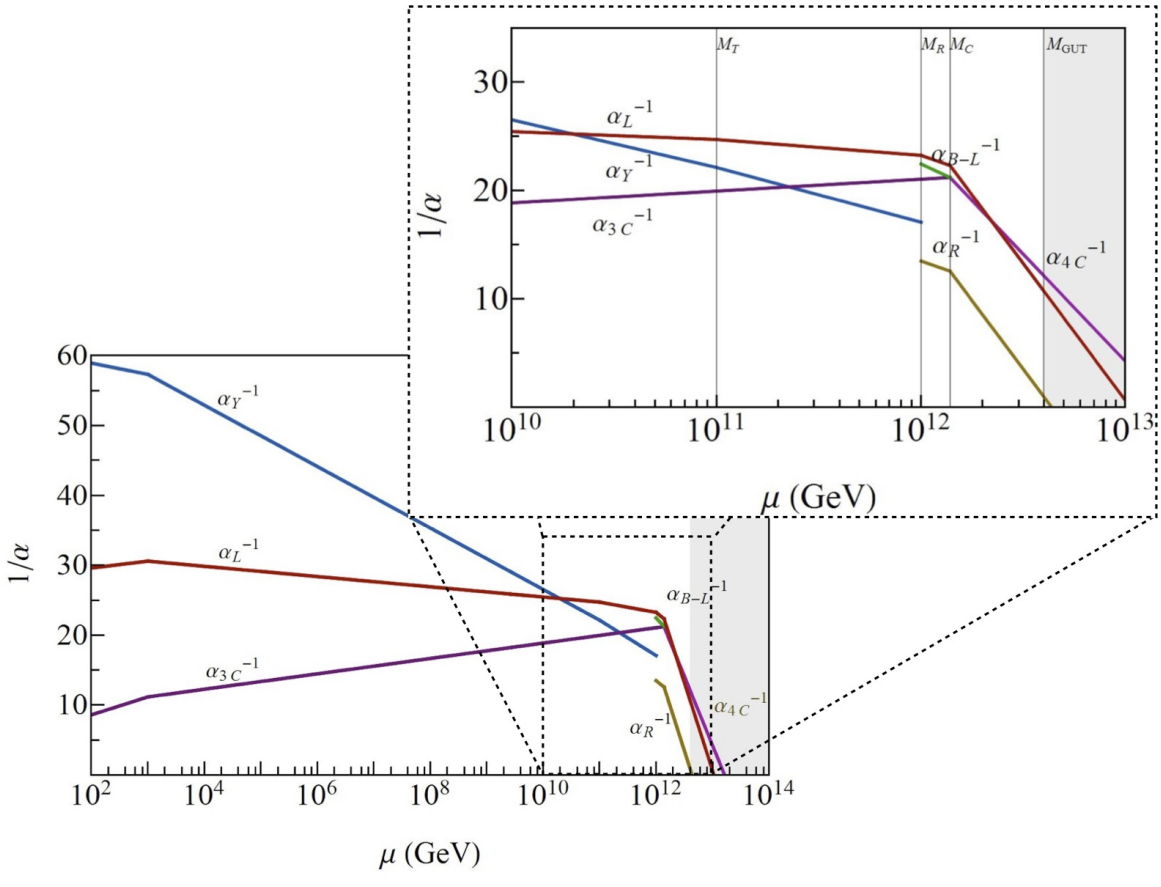

Figure 4.7: *The running of the gauge coupling constants in the more constraining approach.* $M_T = 10^{11}$ *GeV,* $M_R = 10^{12}$ *GeV,* $M_C = 1.4 \times 10^{12}$ *GeV (where* $\alpha_R = 1/4\pi$*) and* $M_{gut} = 4.0 \times 10^{12}$ *GeV (where* $\alpha_R = 1$*). In the dotted figure, we show a detail of the full plot, restricting the energy scale inside the range* $10^{10} \div 10^{13}$ *GeV.*

RGEs of the model presented is beyond the purpose of this work. For this reason we neither run the parameters of the scalar superpotential nor include and run the parameters of the soft SUSY breaking potential. Under these approximations the EW vacuum expectation values do not change from the GUT scale down to the EW one. However this does not affect our conclusions for what concerns the stability of the mass matrix structures since the EW vev shifts due to the running factorize out and leave the Yukawa flavour structure unchanged. The study of the Yukawa matrix running is done in the next section.

4.10 Running of the Yukawa couplings

In the previous section we analyzed the constraints on the scalar Higgs sector coming from the requirement of type-II seesaw dominance and from the presence of the flavour symmetry under which the Higgs fields non-trivially transform. We found that the model is viable only in a small region of the parameter space for which M_R, M_C and $M_{GUT} \sim 10^{13}$ GeV are very close to each other. At the same time M_T lies at only one order of magnitude below M_R. For these reasons to study the stability of the flavour structure of the fermion mass matrices at low scale we can consider only the running from M_T onwards, thus neglecting the running from higher energies. Furthermore we also neglect the running from $M_{\rm susy}$ to the EW scale, which would introduce only minor corrections. We work under the assumption that type-II seesaw is dominating over type-I and moreover that the

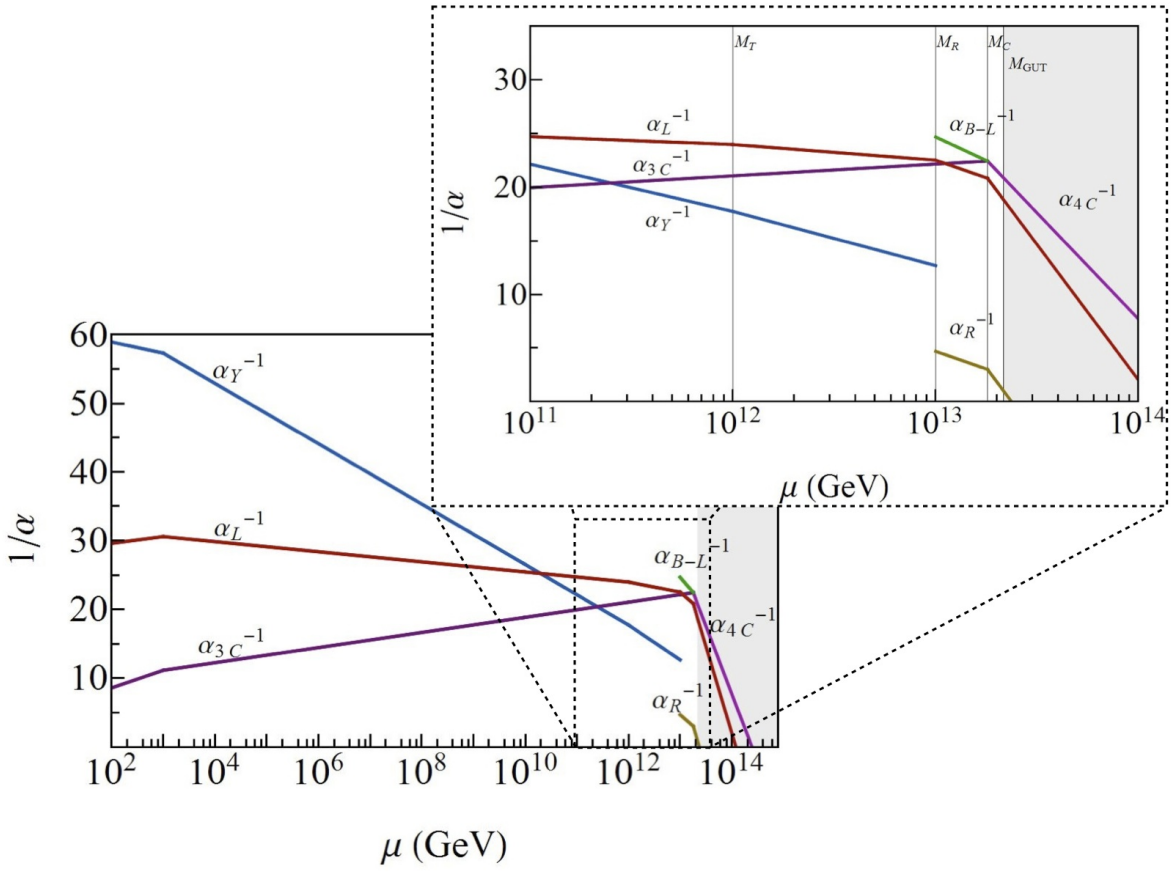

Figure 4.8: *The running of the gauge coupling constants in the less constraining approach.* $M_T = 10^{12}$ *GeV,* $M_R = 10^{13}$ *GeV,* $M_C = 1.8 \times 10^{13}$ *GeV (where* $\alpha_R = 1/3$*) and* $M_{gut} = 2.2 \times 10^{13}$ *GeV (where* $\alpha_R = 1$*). In the dotted figure, we show a detail of the full plot, restricting the energy scale inside the range* $10^{11} \div 10^{14}$ *GeV.*

effects from the type-I terms under the RGEs are negligible. Therefore, when studying the running of the Yukawa couplings, we do not take into account the Weinberg operator originating by integrating out the right-handed neutrinos. The error we introduce in this way is less than λ^2 and we will see in a while that these contributions do not modify our results. Furthermore, we study the stability under the Renormalization Group (RG) running in the approximation corresponding to the NLO, i.e. considering the mass matrices introduced in equations (4.46)–(4.48).

4.10.1 Yukawa matrices at M_T

We start the renormalization group running at M_T; at this scale we integrate out the $SU(2)_L$ scalar triplet T obtaining an effective Weinberg operator responsible of the type-II seesaw contribution. The origin of this effective operator is in the Majorana parts of the matter superpotential given in (4.31) and (4.51), that contain terms with the coupling

$$F_L F_L \Delta_L \ . \tag{4.77}$$

The scalar part of the superpotential (4.74) contains the terms

$$\begin{aligned}&\frac{1}{2}\lambda_{\phi\Sigma}\phi\phi\Sigma+\frac{1}{2}\lambda_{\phi'\Sigma}\phi'\phi'\Sigma+\lambda_{\phi\phi\Sigma}\phi'\phi\Sigma+\frac{1}{2}\lambda_{\rho\Sigma}\rho\rho\Sigma+\\&+\lambda_{\Delta\Sigma'}\Delta_L\overline{\Delta}_R\Sigma'+\overline{\lambda}_{\Delta\Sigma'}\Delta_R\overline{\Delta}_L\Sigma'+\frac{1}{3}\lambda_{\Sigma}\Sigma\Sigma\Sigma+\frac{1}{2}\lambda_{\Sigma'}\Sigma'\Sigma'\Sigma\,.\end{aligned}\tag{4.78}$$

These terms ensure the mixing between the (1,3,1) ((1,3,-1)) components of Δ_L ($\overline{\Delta}_L$), Σ and Σ', whose lighter combination is identified with T ($\overline{T}$), and provides the coupling of T ($\overline{T}$) with the light doublets h_d and h'_d (h_u and h'_u). The effective Weinberg operator at M_T is given by

$$\alpha_{ij}Y_{L_{rs}}\,\frac{L_rL_sh_{u_i}h_{u_j}}{M_T}\,.\tag{4.79}$$

Here L_i represents the $SU(2)_L$ lepton doublets; $h_{u_1}=h_u$, $h_{u_2}=h'_u$ and α_{ij} are coefficients arising by the scalar potential whilst Y_L is given by 4.53 without terms of order λ^3, that we neglect because they are irrelevant for the following analysis.

$$Y_L=\begin{pmatrix}k'_0 & k'_1\lambda & 0\\ k'_1\lambda & k'_0 & 0\\ 0 & 0 & k'_0+k'_2\lambda^2\end{pmatrix}\,.\tag{4.80}$$

The Dirac part of the superpotential at M_T is written as a function of the charged fermion Yukawa matrices and the low energy Higgs fields $h_{u,d}$ and $h'_{u,d}$.

$$Y_uQ\,U^ch_u+Y'_uQ\,U^ch'_u+Y_dQ\,D^ch_d+Y'_dQ\,D^ch'_d+Y_eL\,E^ch_d+Y'_eL\,E^ch'_d\,.\tag{4.81}$$

These matrices have the same textures as their counterparts (4.46) –(4.48), but we absorb a factor of λ

$$\begin{aligned}Y_u&=\frac{1}{\beta}Y'_u=\begin{pmatrix}0 & \tilde{y}_8\lambda^5 & \tilde{y}_6\lambda\\ \tilde{y}_5\lambda^6 & \tilde{y}_3\lambda^4 & \tilde{y}_1\\ \tilde{y}_{10}\lambda^6 & -\tilde{y}_3\lambda^4 & \tilde{y}_1\end{pmatrix}\,,\\ Y_d&=U_{13}\begin{pmatrix}0 & \tilde{y}_7\lambda & 0\\ \tilde{y}_4\lambda^2 & \tilde{y}_2 & 0\\ \tilde{y}_9\lambda^2 & -\tilde{y}_2 & 0\end{pmatrix}\lambda^2+\begin{pmatrix}0 & 0 & \tilde{y}_6\lambda\\ 0 & 0 & \tilde{y}_1\\ 0 & 0 & \tilde{y}_1\end{pmatrix}\,,\\ Y'_d&=U_{23}\begin{pmatrix}0 & \tilde{y}_7\lambda & 0\\ \tilde{y}_4\lambda^2 & \tilde{y}_2 & 0\\ \tilde{y}_9\lambda^2 & -\tilde{y}_2 & 0\end{pmatrix}\lambda^2+\beta\begin{pmatrix}0 & 0 & \tilde{y}_6\lambda\\ 0 & 0 & \tilde{y}_1\\ 0 & 0 & \tilde{y}_1\end{pmatrix}\,,\\ Y_e&=-3U_{13}\begin{pmatrix}0 & \tilde{y}_7\lambda & 0\\ \tilde{y}_4\lambda^2 & \tilde{y}_2 & 0\\ \tilde{y}_9\lambda^2 & -\tilde{y}_2 & 0\end{pmatrix}\lambda^2+\begin{pmatrix}0 & 0 & \tilde{y}_6\lambda\\ 0 & 0 & \tilde{y}_1\\ 0 & 0 & \tilde{y}_1\end{pmatrix}\,,\\ Y'_e&=-3U_{23}\begin{pmatrix}0 & \tilde{y}_7\lambda & 0\\ \tilde{y}_4\lambda^2 & \tilde{y}_2 & 0\\ \tilde{y}_9\lambda^2 & -\tilde{y}_2 & 0\end{pmatrix}\lambda^2+\beta\begin{pmatrix}0 & 0 & \tilde{y}_6\lambda\\ 0 & 0 & \tilde{y}_1\\ 0 & 0 & \tilde{y}_1\end{pmatrix}\,.\end{aligned}\tag{4.82}$$

The U matrix defines the light $SU(2)_L$ Higgses in term of the PS Higgs field components, as explicitly written in appendix 4.A while $\tilde{y}_i$ has to be read as $U_{11}\tilde{y}_i^{(1)}+U_{12}\tilde{y}_i^{(2)}$ and $\beta\tilde{y}_i$ as $U_{21}\tilde{y}_i^{(1)}+U_{22}\tilde{y}_i^{(2)}$.

4.10.2 Analytical approximations

In the appendix 4.D, we report all the RGEs for the Yukawa matrices, while here we discuss the results. The RGEs present the general compact expressions

$$\begin{aligned}
\frac{dY_L}{dt'} &= \mathcal{F}_L\left[Y_{f'}Y_{f'}^\dagger\right]Y_L + Y_L\mathcal{F}_L^T\left[Y_{f'}Y_{f'}^\dagger\right] + \left[\mathcal{G}_\mathcal{L}\left[\mathrm{Tr}(Y_{f'}Y_{f'}^\dagger)\right] - \sum_i c_i^\nu g_i^2\right]Y_L\,, \\
\frac{dY_f}{dt'} &= \mathcal{F}_f\left[Y_{f'}Y_{f'}^\dagger\right]Y_f + \left[\mathcal{G}_f\left[\mathrm{Tr}(Y_{f'}Y_{f'}^\dagger)\right] - \sum c_i^f g_i^2\right]Y_f\,.
\end{aligned} \tag{4.83}$$

In these equations the index f runs over $\{e,u,d\}$; the parameter t' is defined as $t' \equiv t/(16\pi^2) \equiv \log\mu/(16\pi^2)$; $\mathcal{F}_X\left[\ldots\right]$ is a matrix written in terms of the fermion Yukawa matrices $Y_{f'}$; $\mathcal{G}_X\left[\ldots\right]$ is function of the trace in the flavour space over the Yukawa matrices $Y_{f'}$ and c_i^f are the Casimir coefficients related to the group representations (see appendix 4.D for the details). The generic solutions are given by

$$\begin{aligned}
Y_L(\mu) \sim \prod_i e^{-c_i^\nu\mathcal{I}_i} &\times \exp\left[\int_{t'(\mu_0)}^{t'(\mu)}\mathcal{G}_L\left[\mathrm{Tr}(Y_{f'}Y_{f'}^\dagger)\right]dt'\right]\times\exp\left[\int_{t'(\mu_0)}^{t'(\mu)}\mathcal{F}_L\left[Y_{f'}Y_{f'}^\dagger\right]dt'\right] \\
&\times Y_L(\mu_0)\times\exp\left[\int_{t'(\mu_0)}^{t'(\mu)}\mathcal{F}_L^T\left[Y_{f'}Y_{f'}^\dagger\right]dt'\right]\,, \\
Y_f(\mu) = \prod_i e^{-c_i^f\mathcal{I}_i} &\times \exp\left[\int_{t'(\mu_0)}^{t'(\mu)}\mathcal{G}_f\left[\mathrm{Tr}(Y_{f'}Y_{f'}^\dagger)\right]dt'\right]\times\exp\left[\int_{t'(\mu_0)}^{t'(\mu)}\mathcal{F}_f\left[Y_{f'}Y_{f'}^\dagger\right]dt'\right] \\
&\times Y_f(\mu_0)\,.
\end{aligned} \tag{4.84}$$

Here $\mathcal{I}_i = \int_{t'(\mu_0)}^{t'(\mu)} g_i(t')^2 dt'$. When we fix $\mu_0 \sim M_T$ and $\mu \sim M_{\rm susy}$ these formulas can be approximated as functions of $\Delta t' = 1/16\pi^2\log(M_{\rm susy}/M_T) \approx 0.13$

$$\begin{aligned}
Y_L(M_{\rm susy}) &\simeq \left(1 + \mathcal{G}_L\left[\mathrm{Tr}(Y_{f'}Y_{f'}^\dagger)\right]\Delta t' - \sum_i c_i^\nu\mathcal{I}_i\right)Y_L(M_T) + \\
&+ \left(\mathcal{F}_L\left[Y_{f'}Y_{f'}^\dagger\right]Y_L(M_T) + Y_L(M_T)\mathcal{F}_L^T\left[Y_{f'}Y_{f'}^\dagger\right]\right)\Delta t'\,, \\
Y_f(M_{\rm susy}) &\simeq \left(1 + \mathcal{G}_f\left[\mathrm{Tr}(Y_{f'}Y_{f'}^\dagger)\right]\Delta t' - \sum_i c_i^f\mathcal{I}_i\right)Y_f(M_T) + \mathcal{F}_f\left[Y_{f'}Y_{f'}^\dagger\right]Y_f(M_T)\,\Delta t'\,.
\end{aligned} \tag{4.85}$$

In the quark sector we find the following approximate expressions for the masses of the last two families and the Cabibbo angle

$$\begin{aligned}
m_t^2(M_{\rm susy}) &\sim m_t^2\left(1 - 2\textstyle\sum_i c_i^u\,\mathcal{I}_i + 14\,\gamma\,\Delta t'\right)\,, \\
m_c^2(M_{\rm susy}) &\sim m_c^2\left(1 - 2\textstyle\sum_i c_i^u\,\mathcal{I}_i + 6\,\gamma\,\Delta t'\right)\,, \\
m_b^2(M_{\rm susy}) &\sim m_b^2\left(1 - 2\textstyle\sum_i c_i^d\,\mathcal{I}_i + 16\,\gamma\,\Delta t'\right)\,, \\
m_s^2(M_{\rm susy}) &\sim m_s^2\left(1 - 2\textstyle\sum_i c_i^d\,\mathcal{I}_i + 8\,\gamma\,\Delta t'\right)\,, \\
\theta_{12}^q(M_{\rm susy}) &\sim \theta_{12}^q + \frac{1}{6\sqrt{2}}U_{13}^2\,\lambda\,\Delta t'\,.
\end{aligned} \tag{4.86}$$

Here $\gamma = m_t^2/(v_1^u + \beta v_2^u)^2$ and the masses and the Cabibbo angle on the right of the previous expressions are intended at the M_T scale. Note that the demand that m_b^2 is still positive at $M_{\rm susy}$ gives a lower bound on γ of 0.7. The charged lepton masses are very similar to the down-quark masses and indeed we have

$$\begin{aligned}
m_\tau^2(M_{\rm susy}) &\sim m_\tau^2\left(1 - 2\textstyle\sum_i c_i^e\,\mathcal{I}_i + 16\,\gamma\,\Delta t'\right)\,, \\
m_\mu^2(M_{\rm susy}) &\sim m_\mu^2\left(1 - 2\textstyle\sum_i c_i^e\,\mathcal{I}_i + 8\,\gamma\,\Delta t'\right)\,.
\end{aligned} \tag{4.87}$$

We now consider the neutrino sector (see [112–119] for a general approach to RGEs with or without flavour symmetries) and the modification due to the RG running. We recall that our model at the GUT scale naturally predicts the quasi degenerate (QD) spectrum, with both normal and inverse ordering, while choosing a less natural range of the parameters space we may have both the normal hierarchy (NH) and the inverted hierarchy (IH). To simplify the analysis of the effect of the RGEs on the neutrino mass matrix M_ν, we rotate M_ν by a maximal rotation in the $(1\ 2)$ sector. Then, at the high scale, M_ν is diagonal and reads as

$$M_\nu = \begin{pmatrix} k'_0 - \lambda k'_1 & 0 & 0 \\ 0 & k'_0 + \lambda k'_1 & 0 \\ 0 & 0 & k'_0 + \lambda^2 k'_2 \end{pmatrix} v_L \,. \tag{4.88}$$

Without loss of generality k'_0 can be taken real, by a redefinition on the phases. After the running at M_{susy} equation (4.88) gets a correction ΔM_ν. The form of this correction depends on the neutrino hierarchy. For the quasi-degenerate hierarchy and the inverse hierarchy (when $k'_2 \sim \mathcal{O}(1)$, it reads as follows (with $w_\pm = (\pm\gamma/\sqrt{2} + \sqrt{2}\lambda)$)

$$\begin{aligned} \frac{\Delta M_\nu}{v_L} \sim & \left(-k'_0 \sum_i c_i^\nu \mathcal{I}_i + \frac{13}{2} k'_0 \gamma\, \Delta t' \right) \mathbb{1} + \sum_i c_i^\nu \mathcal{I}_i \begin{pmatrix} \lambda k'_1 & 0 & 0 \\ 0 & -\lambda k'_1 & 0 \\ 0 & 0 & 0 \end{pmatrix} + \\ & + \Delta t' \begin{pmatrix} -2\lambda k'_0 - 13\lambda k'_1 \gamma/2 & -k'_0\gamma/2 & k'_0 w_- + k'_1 \lambda\gamma/2\sqrt{2} \\ -k'_0\gamma/2 & 2\lambda k'_0 + 13\lambda k'_1\gamma/2 & k'_0 w_+ + k'_1\lambda\gamma/2\sqrt{2} \\ k'_0 w_- + k'_1\lambda\gamma/2\sqrt{2} & k'_0 w_+ + k'_1\lambda\gamma/2\sqrt{2} & 7\gamma k'_0 \end{pmatrix} . \end{aligned} \tag{4.89}$$

For the normal hierarchy case characterized by $k'_2 \sim \lambda^{-2}$, ΔM_ν assumes the following form

$$\begin{aligned} \frac{\Delta M_\nu}{v_L} \sim & \left(-k'_0 \sum_i c_i^\nu \mathcal{I}_i + \frac{13}{2} k'_0 \gamma\, \Delta t' \right) \mathbb{1} + \sum_i c_i^\nu \mathcal{I}_i \begin{pmatrix} \lambda k'_1 & 0 & 0 \\ 0 & -\lambda k'_1 & 0 \\ 0 & 0 & -\lambda^2 k'_2 \end{pmatrix} + \\ & + \Delta t' \begin{pmatrix} -2\lambda k'_0 - 13\lambda k'_1 \gamma/2 & -k'_0\gamma/2 & k'_0 w_- + k'_-\gamma/2\sqrt{2} \\ -k'_0\gamma/2 & 2\lambda k'_0 + 13\lambda k'_1\gamma/2 & k'_0 w_+ + k'_+\gamma/2\sqrt{2} \\ k'_0 w_- + k'_-\gamma/2\sqrt{2} & k'_0 w_+ + k'_+\gamma/2\sqrt{2} & 7\gamma(k'_0 + k'_2\lambda^2) \end{pmatrix} . \end{aligned} \tag{4.90}$$

Here $k'_\pm$ is given by $(k'_1\lambda \pm k'_2\lambda^2)$.

We can now consider the three different cases QD, NH and IH, which the model accounts for at the GUT scale.

- QD case $\Longrightarrow k'_0, k'_1, k'_2 \sim \mathcal{O}(1)$.
  The correction given by the running induces a rotation in the (23) sector characterized by

$$\tan 2\theta_{23}^\nu \sim -\frac{\sqrt{2}\Delta t'}{\lambda} \frac{k'_0}{|k'_1|}\gamma \sim -2\sqrt{2}\lambda \frac{k'_0}{|k'_1|}\gamma \,. \tag{4.91}$$

  The last equality follows from $\Delta t' \sim 2\lambda^2$. This is a large contribution, which deviates the atmospheric angle from the initial maximal value, spoiling the agreement with the experimental data at 3σ. A possible way out would be if this large correction is erased by a corresponding large correction in the charged lepton mass matrix. However this is not the case, because the maximal θ_{23}^e in the charged lepton mixing matrix is stable under the RG running. As a result, the QD case is not viable. This is an unexpected result. Obviously, the combination of flavour symmetries and grand unified symmetries puts more constraints on model building than naively expected.

- NH case $\Longrightarrow k'_0 \sim \lambda^2$, $k'_1 \sim \mathcal{O}(1)$ and $k'_2 \sim \lambda^{-2}$.
  The corrections both to the atmospheric and to the reactor angles are of order $\Delta t'\gamma/2\sqrt{2} \sim 3\lambda^3$ and can be safely neglected. Analogously, also the mass splittings receive deviations which can be neglected. On the other hand, the charged lepton mixing matrix is stable under the RG running. As a result the three mixing angles at M_{susy} can be well approximated with their initial values at M_T.

- First IH case $\Longrightarrow k'_0 \sim \lambda^2$ and $k'_1, k'_2 \sim \mathcal{O}(1)$.
  All the corrections to the neutrino mixing are of order $\gamma\Delta t'/\sqrt{2}$. While the solar mass splitting receives negligible contributions, the atmospheric mass splitting is corrected as follows

$$\Delta m^2_{atm}(M_{\text{susy}}) = \Delta m^2_{atm}\left(1 - 2\sum_i c^\nu_i \mathcal{I}_i + 13\,\gamma\,\Delta t'\right) . \tag{4.92}$$

  Corrections to the mixing angles coming from the RG running are proportional to $\Delta t'$. At this order of approximation, the corrections to $\theta^l_{12}(M_{\text{susy}})$ and $\theta^l_{13}(M_{\text{susy}})$ come from the charged lepton sector, while that one to $\theta^l_{23}(M_{\text{susy}})$ arises only by the neutrino sector. The resulting mixing angles at the susy scale are

$$\begin{aligned}
\theta^l_{12}(M_{\text{susy}}) &\sim \pi/4 - \theta^e_{12} + \theta^e_{13}\gamma/2\Delta t' , \\
\theta^l_{23}(M_{\text{susy}}) &\sim \theta^e_{23} + \gamma\Delta t' , \\
\theta^l_{13}(M_{\text{susy}}) &\sim \theta^e_{13} - \theta^e_{12}\gamma/2\Delta t' .
\end{aligned} \tag{4.93}$$

  These corrections are more significant than those of the NH case, but their magnitude is small enough to consider the mixing pattern still viable. In this scenario, we only used one 'unnatural' parameter ($k'_0 \sim \lambda^2$), while the NH case has two (one of order λ^2 and one of order λ^{-2}). We can thus conclude that after the dismissal of the QD scenario, the appearance of the inverse hierarchy with neutrino observables as above is a (weak) prediction of our model.

- Second IH case $\Longrightarrow k'_2 \sim \lambda^2$, $k'_0 \sim 1$ and $k'_1 \sim \lambda^{-1}$.
  We recover the same shifts as in the previous case for the atmospheric mass splitting and the lepton mixing angles. The difference lies in the fact that also the solar mass splitting gets a non-negligible correction

$$\Delta m^2_{sol}(M_{\text{susy}}) = \Delta m^2_{sol}\,(1 - 2\textstyle\sum_i c^\nu_i\,\mathcal{I}_i + 14\,\gamma\,\Delta t') . \tag{4.94}$$

  This scenario is thus also possible, but slightly disfavoured with respect to the previous one.

We conclude this section by re-stating the important conclusion. Due to interference between the flavour and the grand unified symmetry, the Yukawa coupling running from the GUT scale (or from the type-II seesaw scale) to a low scale has important effects. These effects are strongest in the quasi-degenerate case and we have seen that agreement with the data cannot support this shift. As a result, only the normal and inverse hierarchy are feasible, with the latter slightly preferred. In the next section we study the phenomenological consequences for the neutrino sector.

4.11 Neutrino Phenomenological Analysis

In the previous section, it was concluded that the quasi-degenerate spectrum is unstable under the RG running and becomes phenomenologically inviable due to too large corrections to the atmospheric mixing angle. Only the normal and inverse hierarchies were shown to be stable and phenomenologically viable. This is different from [64], where only the normal hierarchy and the quasi-degenerate spectrum with normal ordering were found.

In this section, we discuss neutrino phenomenology in more detail, focussing on the value of the reactor mixing angle θ^l_{13} and the possibility of neutrinoless double beta decay.

The analytical expression of the reactor mixing angle is given by equation (4.63) at NLO and it is corrected by the RG running as in equation (4.93) for the two IH scenarios studied in the previous section. We see that θ^l_{13} is typically of order $\lambda \approx 0.2$, so $\sin^2\theta^l_{13} \approx 0.04$. This is rather large: approximately at the $+2\sigma$ level according to [24], so still viable and values of θ^l_{13} just slightly smaller fit the central region very well. This is both true for the current data and for the data at the time when the model was first written down [22, 23].

Here, we complete the study of θ_{13}^l, performing a numerical analysis and comparing it with (the errors on) the data. As can be seen from equations (4.46)–(4.53), the neutrino and the charged lepton mass matrices at NLO are functions of many parameters. However the GUT nature of the model allows us to fix most parameters that occur at LO because they enter in the low energy expressions for quark and charged lepton masses, as can been seen comparing equation (4.26) with (4.86). Note that all dimensionless parameters, i.e. the $\tilde{y}_i$, can be fixed to be of order 1.

The other free parameters can be fixed as random numbers of order 1, except for the cases where we have argued in the previous section that they should have slightly larger or smaller values. Because of the use of random numbers, the predictions of our model are no longer single valued.

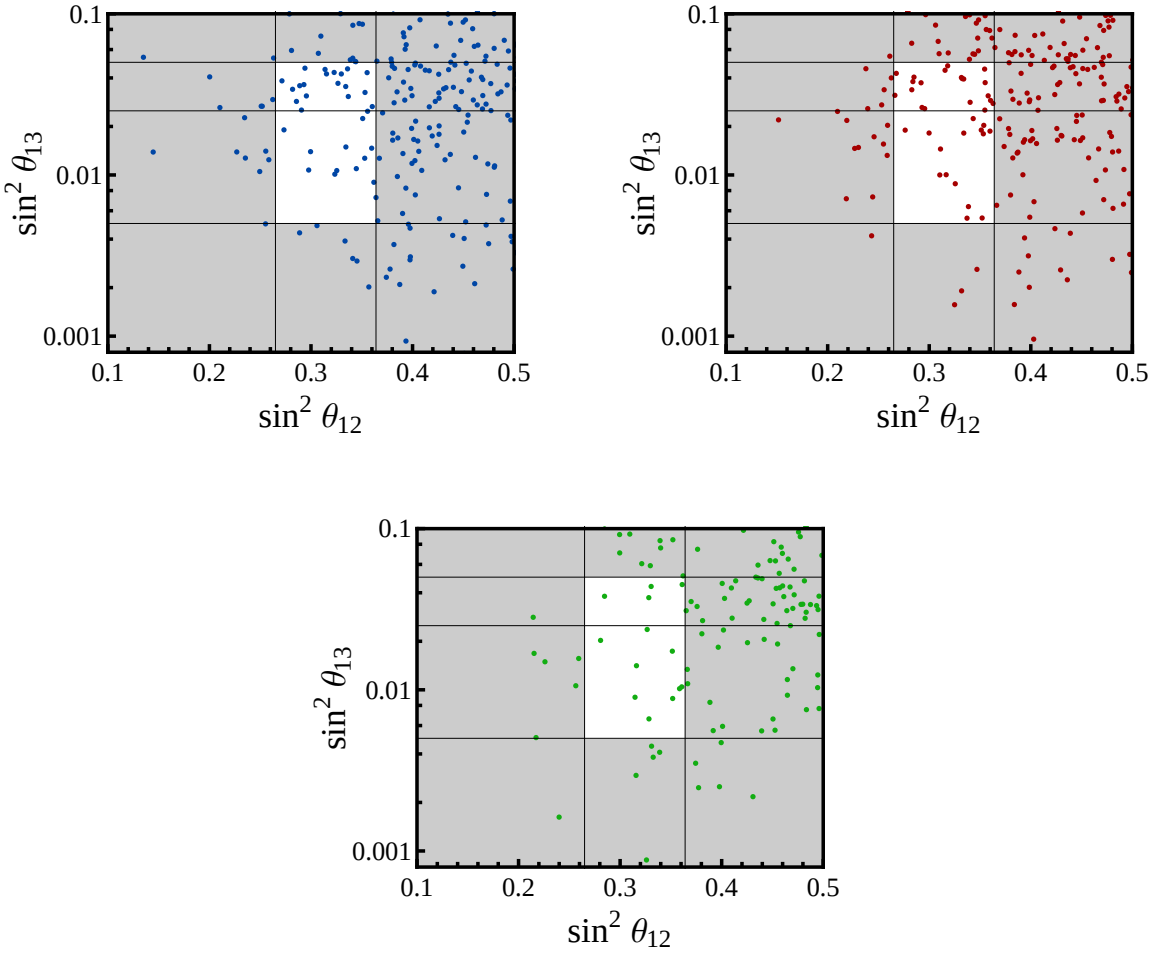

Figure 4.9: The solar angle versus the reactor angle. On the upper line the two IH cases of the previous section (on the left the first case and on the right the second one), while on the lower line the NH one. The two vertical lines are the 3σ bounds for $\sin^2\theta_{12}^l$ according to [24]. The upper horizontal line is the 3σ upper bound for $\sin^2\theta_{13}^l$ and the middle line is the best fit value and the lower line is the 3σ lower bound.

We plot the reactor angle versus the solar angle in figure 4.9. At NLO, equation (4.64), θ_{12}^l is driven away from the maximal value $\pi/4$ by a term proportional to λ (note that we take only the corrections which decrease the value of the solar angle, neglecting those which increase it). We see that this deviation is not for all values of the parameters large enough to bring it in the observed region, although this happens for a significant number of them. As explained above, larger values of $\sin^2\theta_{13}^l$ are favoured and almost all points are in the sensitive region for experiments.

To study neutrinoless double beta decay, we consider the effective $0\nu\beta\beta$ parameter m_{ee}, defined as

$$m_{ee} = [U \,\mathrm{diag}(m_1,\, m_2,\, m_3)\, U]_{11}. \tag{4.95}$$

In figure 4.10 we plot m_{ee} against the lightest neutrino mass, which is m_1 and m_3 in the NH and IH case respectively. The future experiments are expected to reach good sensitivities: 90 meV [30] (GERDA), 20 meV [31] (Majorana), 50 meV [32] (SuperNEMO), 15 meV [33] (CUORE) and 24 meV [34] (EXO). As a result, looking at figure 4.10, the whole IH band will be tested in the next future and with it the two cases of our model which allow for the IH spectrum.

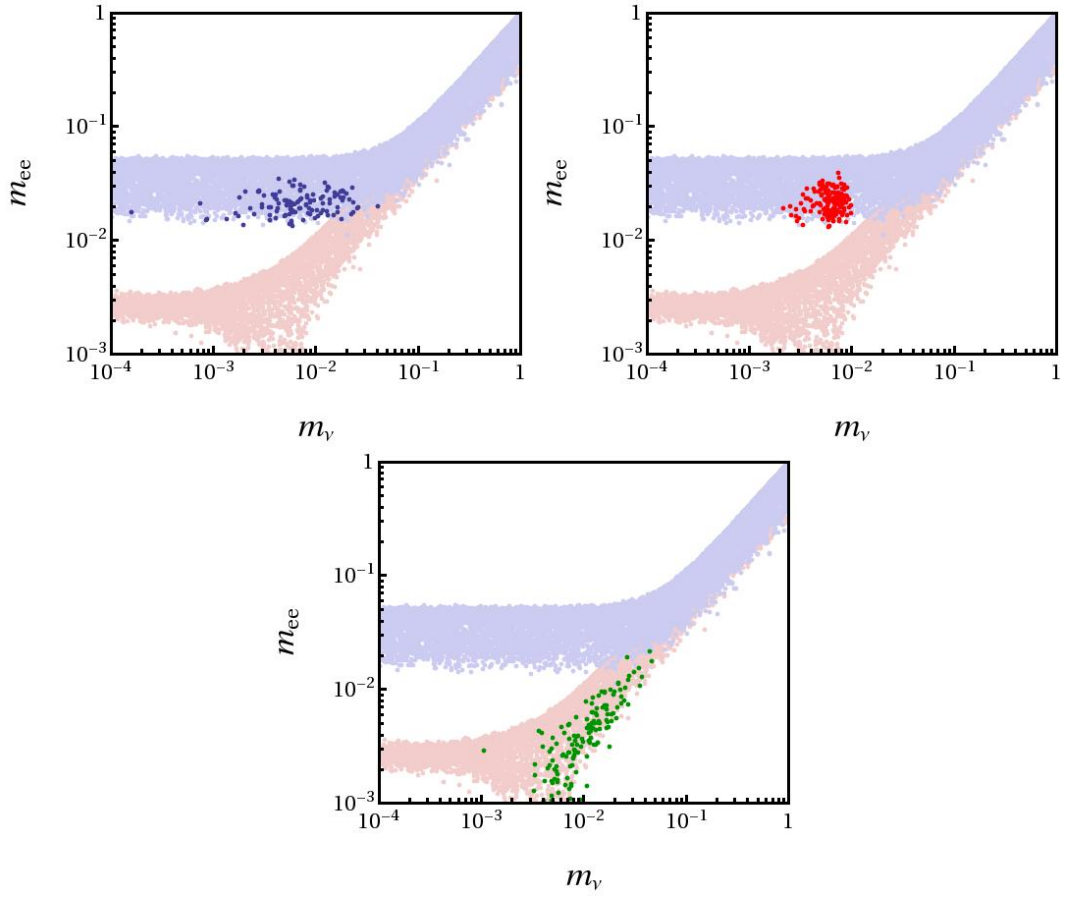

Figure 4.10: *Neutrinoless double beta decay plots. On the upper line the two IH cases of the previous section (on the left the first case and on the right the second one), while on the lower line the NH one. The background red (blue) points refer to the allowed region for the NH (IH), taking into account the lepton mixing angle values with their 3σ errors.*

4.12 Conclusions of the chapter

In this chapter we have addressed several aspects of the interplay between a GUT based model and a discrete flavour symmetry. The chapter should indeed be considered as the combination of three distinct parts: it starts with a part in which many concepts and motivations are introduced. In the second one we mainly discussed the building of the model from the flavour point of view, while in the last one we faced the problem to justify the assumptions made in the second part and to achieve the correct gauge symmetry breaking chain. We found that this gives non-trivial constraints on the model building.

More in detail, the symmetry group of our model is $PS \times G_f$, where PS stands for the GUT Pati–Salam gauge group $SU(4)_C \times SU(2)_L \times SU(2)_R$ and G_f for the flavour group $S_4 \times Z_4 \times U(1)_{FN} \times U(1)_R$. Within this GUT context one has the relationship between the down-quark and charged leptons mass matrices, $M_d \sim M_e$, which can easily be used to revise the old idea of quark-lepton complementarity. In the model this is obtained by the use of the non-Abelian discrete flavour symmetry S_4 properly broken through the vevs of a set of flavon fields, which transform as triplets under S_4. The additional Abelian symmetries, which enters in G_f, play different roles: Z_4 keeps quarks separated from leptons and neutrinos from charged leptons and prevents dangerous couplings in the superpotential of the model; $U(1)_{FN}$ helps to justify the charged fermion mass hierarchies; $U(1)_R$ is a common ingredient of supersymmetric flavour models. It contains the discrete R-parity and is useful to build a suitable flavon superpotential that allows the correct S_4 breaking pattern.

Already at the leading order, the model shows nice features: we are able to reproduce the mass hierarchy between the third and the second charged fermion families, the bottom-tau unification, the Georgi–Jarlskog [99] relation $|m_\mu| = 3|m_s|$ and, under the assumption of type-II seesaw dominance at the GUT scale, a realistic neutrino spectrum. However at this level of approximation, both the CKM and the PMNS mixing matrices are not correct: the quark mixing matrix coincides with the identity matrix, while the lepton one is given by the BM pattern. It is worth to recall here that the BM mixing corresponds to maximal solar and atmospheric angles and to a vanishing reactor angle: only the solar angle is not in agreement with the data as it deviates from the experimental central value by a quantity close to the Cabibbo angle, $\lambda \sim 0.2$.

At next-to-leading order, the wrong predictions for the fermion mixing angles are corrected: in the CKM matrix, the mixing angle θ^q_{12} receives contributions of the order of λ, fitting the value of the Cabibbo angle; analogously, in the PMNS matrix, the solar angle is corrected by the same amount and we find the nice result that $\theta^l_{12} \sim \pi/4 - \mathcal{O}(\lambda)$. At the same time, also the reactor angle receives significant contributions and indeed at this level of approximation it results $\theta^l_{13} \sim \mathcal{O}(\lambda)$: this is an interesting feature of our model, this value is close to the experimental upper bound at the time the model was constructed and indeed this prediction seems confirmed by more recent data. It will further be tested in the forthcoming neutrino experiments [42–45, 120–123].

Once we consider the higher order terms, we find the other two CKM angles of the correct order of magnitude, $\theta^q_{23} \sim \mathcal{O}(\lambda^2)$ and $\theta^q_{13} \sim \mathcal{O}(\lambda^3)$, and small corrections are introduced in the PMNS angles: in particular the atmospheric angle becomes $\theta^l_{23} \sim \pi/4 + \mathcal{O}(\lambda^2)$, justifying a small deviation from the maximality. For what concerns the masses, all the fermions are massive and the mass hierarchies fit the experimental observations.

On the other hand, the neutrino spectrum could be either quasi degenerate or normal or inverse hierarchical. Only the first case corresponds to a completely natural choice of the parameters, which, in the absence of an explanation coming form a higher energy theory, should be of order 1: in order to allow the NH and the IH, the parameters should span in a larger range of values, namely $\lambda^{-2} \div \lambda^2$. In short, the combination of flavour and GUT symmetries allow many observed patterns in the flavour sector to be reproduced. If at this moment a balance had to be made like we did at the end of sections 2.3.1 and 2.4.6, this balance is likely to be positive, or at least as positive as the balances of chapter 2. Our model is slightly larger, but it also explains much more peculiarities of the flavour sector.

In the third part of the chapter (from section 4.9) the tides turned. We have studied the Higgs scalar potential and the running of both the gauge couplings and the Yukawa mass matrices under the RGEs. With this analysis we looked for the constraints which arise to justify the Higgs field vev pattern used in the flavour section and the assumption of the type-II seesaw dominance. The presence of the flavour group G_f modifies the Higgs field content necessary to implement the classical breaking pattern of the PS gauge group and as consequence not all the results obtained by studying minimal versions of PS are recovered. In particular we need the presence of two PS multiplets $(15,1,1)$, A and B, responsible to break the unified colour symmetry $SU(4)_C$ to $SU(3)_C \times U(1)_{B-L}$. Two copies of the $(1,2,2)$ multiplet, ϕ and ϕ', and one $(15,2,2)$ field, ρ, are necessary to implement the condition $v^u_\rho = 0$. Lastly, we need the new fields $\Sigma, \Sigma' \sim (1,3,3)$ and $\xi \sim (1,1,1)$ to have a type-II seesaw contribution at tree level.

The running of the gauge couplings is affected by the large field content and in particular we found that the requirement of having type-II See-Saw dominance constrains the model in a small region of the parameter space, in which all the heavy mass scales are sandwiched between 10^{11} GeV and 10^{13} GeV. At the same time Yukawa mass matrix running shows that while the CKM Cabibbo angle is stable under the RGEs evolution, the PMNS mixing angles are stable only if neutrinos present a NH or an IH spectrum, ruling out the QD case. As already stated, the QD spectrum would be the most natural and probable case at the GUT scale, but the Yukawa RGEs analysis further reduces the allowed region of the parameter space. Whether the negative evidence of the third part of the chapter is enough to swing the balance mentioned above to the negative side (assuming it was positive to start with) is up for everybody's judgement, but it is clear that this evidence should be taken into account in order to form a fair opinion.

In section 4.11, we performed a brief phenomenological analysis of neutrino observables considering all the constraints which come from the flavour and the Higgs sectors. We have first considered the value of the reactor angle in terms of the deviations of the solar angle from the maximal value and the numerical analysis confirmed the analytical results: in our model, θ_{13}^{l} naturally acquires values that more recent data indeed point at. After this, we studied the neutrinoless double beta decay effective mass, m_{ee}, and we have seen that the next future experiments are expected to reach sufficiently good sensitivities to test our model in the IH regime.

The main conclusion of the chapter is that there is a strong tension in combining a GUT model with a (discrete non-Abelian) flavour symmetry and therefore a parallel study is not only interesting but also recommended to provide a viable model. In the second part of the chapter we produced a flavour-GUT model that is quite realistic and viable. Only the study done in the third part, regarding the Higgs sector revealed that the model is restricted into a small region of the parameter space, reducing the freedom in the choice of the parameter values. Even if our results are model dependent, our construction shares many features with other models present in literature, where often a detailed discussion of the Higgs sector is missing. In our opinion, this is a serious drawback and we would suggest to consider the interplay between GUTs and flavour symmetries in this kind of models as well.

Appendices to chapter 4

4.A Higgs scalar spectrum

In this appendix we present the scalar mass matrices for all the fields introduced in section 4.9 in terms of representations of the SM$\sim SU(3)_C \times SU(2)_L \times U(1)_Y$; we also indicate their origin with respect to the PS and the colour-broken Pati-Salam (CbPS) phase, in which the symmetry group is given by $SU(3)_C \times SU(2)_L \times SU(2)_R \times U(1)_{B-L}$. For completeness for each field we also indicate the corresponding T_{3R} value, with T_{3R} the diagonal generator of $SU(2)_R$. We use the same notation as in [124]: we write the Dirac scalar mass matrices as they could be read directly from the superpotential (4.74) at the scale M_R. We label the mass matrices with S, D and T when they refer to the singlet, doublet and triplet representations respectively of the $SU(2)_L$ gauge symmetry.

Obviously the most interesting subsection of this appendix is 4.A.2 that discusses the colour-singlet $SU(2)$-doublets, that give rise to the light electroweak breaking Higgs fields.

4.A.1 $SU(2)_L$ singlets

We first consider singlets under $SU(2)_L$. When the symmetry breaks down from the Pati-Salam symmetry group to the Standard Model, this $SU(2)_L$ is the only product group that remains unbroken. All Goldstone bosons related to the symmetry breaking chain so far are thus singlets of $SU(2)_L$. In total, the breaking from $SU(4)_C \times SU(2)_L \times SU(2)_R \to SU(3)_C \times SU(2)_L \times U(1)_Y$ should give rise to nine Goldstone bosons. In this appendix, we indeed reproduce these.

• Singlets $(1, 1, 0)$

The mass matrix for the Standard Model singlet scalar fields reads

$$M_{S1} = \begin{pmatrix} 0 & 0 & \frac{3}{\sqrt{2}}\lambda_R M_R & 0 & 0 \\ 0 & 0 & \frac{3}{\sqrt{2}}\lambda_R M_R & 0 & 0 \\ \frac{3}{\sqrt{2}}\lambda_R M_R & \frac{3}{\sqrt{2}}\lambda_R M_R & \sqrt{2}M_{C_1}\lambda_A + x & \lambda_{AB\xi}V_\xi + \frac{1}{\sqrt{2}}\lambda_B M_{C_2} & \frac{1}{\sqrt{2}}\lambda_{AB\xi}M_{C_2} \\ 0 & 0 & \lambda_{AB\xi}V_\xi + \frac{1}{\sqrt{2}}\lambda_B M_{C_2} & \frac{1}{\sqrt{2}}\lambda_{B\xi}M_{C_1} - y & \frac{1}{\sqrt{2}}\lambda_{AB\xi}M_{C_2} \\ 0 & 0 & \frac{1}{\sqrt{2}}\lambda_{AB\xi}M_{C_2} & \frac{1}{\sqrt{2}}\lambda_{AB\xi}M_{C_1} & -\frac{M_{C_1}M_{C_2}}{V_\xi\sqrt{2}}\lambda_{AB\xi} \end{pmatrix} .$$

The parameters x and y are given by

$$x = \frac{1}{2\sqrt{2}M_{C_1}}(-4\lambda_A M_{C_1}^2 - 2\sqrt{2}\lambda_{AB\xi}M_{C_2}V_\xi - 2\lambda_B M_{C_2}^2 - 8\lambda_R M_R^2) ,$$
$$y = \frac{M_{C_1}}{\sqrt{2}M_{C_2}}(\sqrt{2}\lambda_{AB\xi}V_\xi + 2\lambda_B M_{C_2}) .$$

M_{S1} has a vanishing eigenvalue that is eaten by the corresponding gauge boson. Moreover it can be checked that one of the singlets, which we call ξ_0, has a mass $\sim M_R$ while all the others masses appear as combinations of M_{C1}, M_{C2} and V_ξ and are heavier still. We present all states and their origins in the table below.

Field	Origin	PS	CbPS	T_{3R}
C_1, R_1	Δ_R	$(10,1,3)$	$(1,1,3,-2)$	1
C_2, R_2	$\overline{\Delta}_R$	$(\overline{10},1,3)$	$(1,1,3,2)$	-1
C_3, R_3	A	$(15,1,1)$	$(1,1,1,0)$	0
C_4, R_4	B	$(15,1,1)$	$(1,1,1,0)$	0
C_5, R_5	ξ	$(1,1,1)$	$(1,1,1,0)$	0

• **Singlets $(3,1,2/3) \oplus (\overline{3},1,-2/3)$**

$$M_{S2} = \begin{pmatrix} \sqrt{2}\lambda_A M_{C_1} + x & \lambda_{AB\xi} V_\xi + \frac{1}{\sqrt{2}}\lambda_B M_{C_2} & 2\lambda_R M_R \\ \lambda_{AB\xi} V_\xi + \frac{1}{\sqrt{2}}\lambda_B M_{C_2} & \frac{1}{\sqrt{2}}\lambda_B M_{C_1} - y & 0 \\ 2\lambda_R M_R & 0 & -\sqrt{2}\lambda_R M_{C_1} \end{pmatrix} .$$

M_{S2} has a vanishing eigenvalue: it corresponds to the massless GBs $(3,1,2/3) \oplus (\overline{3},1,-2/3)$ eaten by the gauge bosons.

Field	Origin	PS	CbPS	T_{3R}
C_1	A	$(15,1,1)$	$(3,1,1,4/3)$	0
C_2	B	$(15,1,1)$	$(3,1,1,4/3)$	0
C_3	Δ_R	$(10,1,3)$	$(3,1,3,-2/3)$	1
R_1	A	$(15,1,1)$	$(\overline{3},1,1,-4/3)$	0
R_2	B	$(15,1,1)$	$(\overline{3},1,1,-4/3)$	0
R_3	$\overline{\Delta}_R$	$(\overline{10},1,3)$	$(\overline{3},1,3,2/3)$	-1

• **Singlets $(8,1,0)$**

$$M_{S3} = \begin{pmatrix} -\sqrt{2}M_{C1}\lambda_A + x & V_\xi \lambda_{AB\xi} - \frac{1}{\sqrt{2}}\lambda_B M_{C2} \\ V_\xi \lambda_{AB\xi} - \frac{1}{\sqrt{2}}\lambda_B M_{C2} & -\frac{1}{\sqrt{2}}M_{C1}\lambda_B - y \end{pmatrix} .$$

In this case, there are no massless states.

Field	Origin	PS	CbPS	T_{3R}
C_1, R_1	A	$(15,1,1)$	$(8,1,1,0)$	0
C_2, R_2	B	$(15,1,1)$	$(8,1,1,0)$	0

• **Singlets $(1,1,\pm 1)$**

$$M_{S4} = 0 .$$

These states correspond to the last two massless Goldstone bosons eaten by the gauge bosons. With these two states present, the total number of GBs eaten is $1 + 2 \times 3 + 2 = 9$, exactly as required by the symmetry breaking scheme.

Field	Origin	PS	CbPS	T_{3R}
C_1	Δ_R	$(10,1,3)$	$(1,1,3,-2)$	0
R_1	$\overline{\Delta}_R$	$(\overline{10},1,3)$	$(1,1,3,2)$	0

• **Singlets $(1,1,\pm 2)$**

$$M_{S5} = 0 \ .$$

The mass matrix for the colour- and $SU(2)_L$-singlets with hypercharge (and thus electric charge) ± 2 vanishes, implying that these states remain massless until the susy scale, providing a testable prediction of the model (as well as other Pati-Salam set ups). We write these as δ^{++} and $\overline{\delta}^{++}$.

Field	Origin	PS	CbPS	T_{3R}
C_1	Δ_R	$(10,1,3)$	$(1,1,3,-2)$	-1
R_1	$\overline{\Delta}_R$	$(\overline{10},1,3)$	$(1,1,3,2)$	1

• **Singlets $(3,1,-1/3) \oplus (\overline{3},1,1/3)$**

$$M_{S6} = -\sqrt{2} M_{C1} \lambda_R \ .$$

Field	Origin	PS	CbPS	T_{3R}
C_1	Δ_R	$(10,1,3)$	$(3,1,3,-2/3)$	0
R_1	$\overline{\Delta}_R$	$(\overline{10},1,3)$	$(\overline{3},1,3,2/3)$	0

• **Singlets $(3,1,-4/3) \oplus (\overline{3},1,4/3)$**

$$M_{S7} = -\sqrt{2} M_{C1} \lambda_R \ .$$

Field	Origin	PS	CbPS	T_{3R}
C_1	Δ_R	$(10,1,3)$	$(3,1,3,-2/3)$	-1
R_1	$\overline{\Delta}_R$	$(\overline{10},1,3)$	$(\overline{3},1,3,2/3)$	1

• **Singlets $(6,1,4/3) \oplus (\overline{6},1,-4/3)$**

$$M_{S8} = -2\sqrt{2} M_{C1} \lambda_R \ .$$

Field	Origin	PS	CbPS	T_{3R}
C_1	Δ_R	$(10,1,3)$	$(6,1,3,2/3)$	1
R_1	$\overline{\Delta}_R$	$(\overline{10},1,3)$	$(\overline{6},1,3,-2/3)$	-1

• **Singlets $(6,1,1/3)\oplus(\overline{6},1-1/3)$**

$$M_{S9} = -2\sqrt{2}M_{C1}\lambda_R \ .$$

Field	Origin	PS	CbPS	T_{3R}
C_1	Δ_R	$(10,1,3)$	$(6,1,3,2/3)$	0
R_1	$\overline{\Delta}_R$	$(\overline{10},1,3)$	$(\overline{6},1,3,-2/3)$	0

• **Singlets $(6,1,-2/3)\oplus(\overline{6},1,2/3)$**

$$M_{S10} = -2\sqrt{2}M_{C1}\lambda_R \ .$$

Field	Origin	PS	CbPS	T_{3R}
C_1	Δ_R	$(10,1,3)$	$(6,1,3,2/3)$	-1
R_1	$\overline{\Delta}_R$	$(\overline{10},1,3)$	$(\overline{6},1,3,-2/3)$	1

4.A.2 $SU(2)_L$ doublets

Next we consider the $SU(2)_L$ doublets. We start with the doublets that have the right quantum numbers to break electroweak symmetry.

• **Doublets $(1,2,\pm 1/2)$**

The mass matrix relevant for the electroweak-symmetry breaking doublets is

$$M_{D1} = \begin{pmatrix} M_\phi & M_{\phi\phi'} & \frac{1}{\sqrt{2}}M_{C2}\lambda_{\phi\rho} \\ M_{\phi\phi'} & M_{\phi'} & \frac{1}{\sqrt{2}}M_{C2}\lambda_{\phi'\rho} \\ \frac{1}{\sqrt{2}}M_{C2}\lambda_{\phi\rho} & \frac{1}{\sqrt{2}}M_{C2}\lambda_{\phi'\rho} & M_\rho + \frac{1}{\sqrt{2}}\lambda_{\rho A}M_{C1} \end{pmatrix} \tag{4.A.1}$$

M_{D1}^2 is diagonalized according to

$$U^T \cdot M_{D1}^2 \cdot U = \hat{M}_{D1}\hat{M}_{D1} \ . \tag{4.A.2}$$

This gives three up-type (down-type) Higgs doublets h_u, h'_u, H_u (h_d, h'_d, H_d) .

$$\begin{pmatrix} \phi_{u,d} \\ \phi'_{u,d} \\ \rho_{u,d} \end{pmatrix} = U^T \begin{pmatrix} h_{u,d} \\ h'_{u,d} \\ H_{u,d} \end{pmatrix} \ . \tag{4.A.3}$$

Therefore for the up (down) projections we have

$$\begin{aligned} v_\phi^{u,d} &\equiv \langle\phi_{u,d}\rangle &&= U_{11}v_1^{u,d} + U_{21}v_2^{u,d} + U_{31}v_3^{u,d} \ , \\ v_{\phi'}^{u,d} &\equiv \left\langle\phi'_{u,d}\right\rangle &&= U_{12}v_1^{u,d} + U_{22}v_2^{u,d} + U_{32}v^{u,d} \ , \\ v_\rho^{u,d} &\equiv \langle\rho_{u,d}\rangle &&= U_{13}v_1^{u,d} + U_{23}v_2^{u,d} + U_{33}v_3^{u,d} \ . \end{aligned} \tag{4.A.4}$$

In general a light doublet, i.e. massless at the M_C scale, gets a mass term at M_{SUSY} and its vev, at the EW scale, is of order of the EW scale $\sim v_W$. On the contrary for a heavy doublet of mass M, its

induced vev at the EW scale is $\sim v_W^2/M$ For $M \sim M_C$ this is completely negligible with respect to v_W.

Consider now the condition $\langle \rho_u \rangle = 0$ that we imposed to get the correct fermion mass matrices. In the standard case we would have only one up- and one down-type light Higgs doublets, with all the other doublets heavy. Assume now that $h_{u,d}$ in equation (4.A.3) are the up- and down-type light doublets at M_C. Then we have $v_1^{u,d} \sim v_W$ while $v_2^{u,d} \sim v_3^{u,d} \sim 0$. From equation (4.A.4) we see that in this case it would be impossible to make the ρ projection vanish along the up-direction (that implies $U_{13} = 0$), while still maintaining a non-vanishing $\langle \rho_d \rangle$.[12] For this reason the condition $\langle \rho_u \rangle = 0$ implies a non-standard scenario and the presence of two light doublets of up-type at the M_C scale, namely h_u and h'_u. However the symmetric nature of M_{D1} ensures that as consequence we are also left with two down-type light Higgs doublets, h_d and h'_d. Nevertheless this does not imply that $\langle \rho_d \rangle$ vanishes because $v_i^{u,d}$ depend on the soft terms and we get

$$\begin{aligned} \langle \rho_u \rangle &= U_{13} v_1^u + U_{23} v_2^u = 0\,, \\ \langle \rho_d \rangle &= U_{13} v_1^d + U_{23} v_2^d \neq 0\,, \end{aligned} \tag{4.A.5}$$

In conclusion we have to impose two constraints on the free parameters that enter in M_{D1} corresponding to require that M_{D1} has two vanishing eigenvalues. Notice that the condition that M_{D_1} has rank 1 is fine-tuned but it is not more fine-tuned than imposing M_{D_1} of rank 2, which is universally accepted whenever the MSSM has to be recovered. In our case the fermion mass matrix structures impose a slightly different condition –M_{D_1} of rank 1 – but both the requirements are satisfied by fine-tuning the parameters that enter in the mass matrix.

Field	Origin	PS	CbPS	T_{3R}
C_1	ϕ	$(1,2,2)$	$(1,2,2,0)$	$1/2$
C_2	ϕ'	$(1,2,2)$	$(1,2,2,0)$	$1/2$
C_3	ρ	$(15,2,2)$	$(1,2,2,0)$	$1/2$
R_1	ϕ	$(1,2,2)$	$(1,2,2,0)$	$-1/2$
R_2	ϕ'	$(1,2,2)$	$(1,2,2,0)$	$-1/2$
R_3	ρ	$(15,2,2)$	$(1,2,2,0)$	$-1/2$

• **Doublets $(\mathbf{3,2,7/6}) \oplus (\overline{\mathbf{3}}\mathbf{,2,-7/6})$**

$$M_{D2} = M_\rho + \frac{1}{\sqrt{2}} \lambda_{\rho A} M_{C_1}\ .$$

Field	Origin	PS	CbPS	T_{3R}
C_1	ρ	$(15,2,2)$	$(3,2,2,4/3)$	$1/2$
R_1	ρ	$(15,2,2)$	$(\overline{3},2,2,-4/3)$	$-1/2$

• **Doublets $(\mathbf{3,2,1/6}) \oplus (\overline{\mathbf{3}}\mathbf{,2,-1/6})$**

$$M_{D3} = M_\rho + \frac{1}{\sqrt{2}} \lambda_{\rho A} M_{C_1}\ .$$

[12] Even the condition $U_{13} = 0$ is not natural. Therefore in the most general case with only one up-type (down-type) light doublet, the condition $\langle \rho_u \rangle = 0$ implies that all the other vevs given in equation (4.A.4) vanish.

Field	Origin	PS	CbPS	T_{3R}
C_1	ρ	$(15,2,2)$	$(3,2,2,4/3)$	$-1/2$
R_1	ρ	$(15,2,2)$	$(\overline{3},2,2,-4/3)$	$1/2$

• **Doublets $(8,2,1/2)\oplus(8,2,-1/2)$**

$$M_{D4} = M_\rho - \frac{1}{\sqrt{2}}\lambda_{\rho A} M_{C_1} \ .$$

Field	Origin	PS	CbPS	T_{3R}
C_1	ρ	$(15,2,2)$	$(8,2,2,0)$	$1/2$
R_1	ρ	$(15,2,2)$	$(8,2,2,0)$	$-1/2$

4.A.3 $SU(2)_L$ triplets

Lastly, we discuss triplets under the Standard Model's $SU(2)_L$.

• **Triplets** $(1,3,1)\oplus(1,3,-1)$

$$M_{T1} = \begin{pmatrix} M_\Sigma & \lambda_\xi V_\xi & 0 \\ \lambda_\xi V_\xi & M_{\Sigma'} & \frac{1}{\sqrt{2}}\lambda M_R \\ 0 & \frac{1}{\sqrt{2}}\overline{\lambda} M_R & M_{\Delta L} + \frac{3}{\sqrt{2}}\lambda_L M_{C_1} \end{pmatrix} .$$

with

Field	Origin	PS	CbPS	T_{3R}
C_1	Σ	$(1,3,3)$	$(1,3,3,0)$	1
C_2	Σ'	$(1,3,3)$	$(1,3,3,0)$	1
C_3	Δ_L	$(\overline{10},3,1)$	$(1,3,1,2)$	0
R_1	Σ	$(1,3,3)$	$(1,3,3,0)$	-1
R_2	Σ'	$(1,3,3)$	$(1,3,3,0)$	-1
R_3	$\overline{\Delta}_L$	$(10,3,1)$	$(1,3,1,-2)$	0

• **Triplets $(1,3,0)$**

$$M_{T2} = \begin{pmatrix} M_\Sigma & \lambda_\xi V_\xi \\ \lambda_\xi V_\xi & M_{\Sigma'} \end{pmatrix} .$$

with

Field	Origin	PS	CbPS	T_{3R}
C_1, R_1	Σ	$(1,3,3)$	$(1,3,3,0)$	0
C_2, R_2	Σ'	$(1,3,3)$	$(1,3,3,0)$	0

• **Triplets $(\mathbf{3, 3, -1/3}) \oplus (\mathbf{\overline{3}, 3, 1/3})$**

$$M_{T3} = M_{\Delta_L} + \frac{1}{\sqrt{2}}\lambda_L M_{C1} \ .$$

with

Field	Origin	PS	CbPS	T_{3R}
C_1	Δ_L	$(\overline{10}, 3, 1)$	$(3, 3, 1, 2/3)$	0
R_1	$\overline{\Delta}_L$	$(10, 3, 1)$	$(\overline{3}, 3, 1, -2/3)$	0

• **Triplets $(\mathbf{6, 3, 1/3}) \oplus (\mathbf{\overline{6}, 3, -1/3})$**

$$M_{T4} = M_{\Delta_L} - \frac{1}{\sqrt{2}}\lambda_L M_{C1}$$

with

Field	Origin	PS	CbPS	T_{3R}
C_1	Δ_L	$(\overline{10}, 3, 1)$	$(6, 3, 1, -2/3)$	0
R_1	$\overline{\Delta}_L$	$(10, 3, 1)$	$(\overline{6}, 3, 1, 2/3)$	0

4.B NLO contributions to the flavon scalar potential

The superpotential w_d of equation (4.71), linear in the driving fields D_R, φ_R, χ_R and σ_R, is modified into:

$$w_d = w_d^0 + \delta w_d \ . \tag{4.B.1}$$

The addition δw_d contains the NLO contributions, suppressed by one power of $1/\Lambda$ with respect to w_d^0; it is given by the most general quartic, $S_4 \times Z_4$-invariant polynomial linear in the driving fields, and can be obtained by inserting an additional flavon field in all the LO terms. The Z_4-charges prevent any addition of the flavons φ and φ' at NLO, while a factor of σ or χ can be added to all the LO terms. The full expression of δw_d is the following:

$$\delta w_d = \frac{1}{\Lambda}\left(\sum_{i=1}^{3} x_i I_i^{\sigma_R} + \sum_{i=1}^{5} w_i I_i^{\chi_R} + \sum_{i=1}^{6} s_i I_i^{D_R} + \sum_{i=1}^{5} v_i I_i^{\varphi_R}\right) \ . \tag{4.B.2}$$

where x_i, w_i, s_i and v_i are coefficients and $\left\{I_i^{\sigma_R},\ I_i^{\chi_R},\ I_i^{D_R},\ I_i^{\varphi_R}\right\}$ represent a basis of independent quartic invariants:

$$\begin{aligned}
&I_1^{\sigma_R} = \sigma_R\sigma\sigma\sigma && I_3^{\sigma_R} = \sigma_R\sigma(\chi\chi)_{1_1} \\
&I_2^{\sigma_R} = \sigma_R(\chi(\chi\chi)_{3_1})_{1_1} && \\
&I_1^{\chi_R} = (\chi_R\chi)_{1_1}(\chi\chi)_{1_1} && I_4^{\chi_R} = (\chi_R(\chi\chi)_{3_1})_{1_1}\,\sigma \\
&I_2^{\chi_R} = ((\chi_R\chi)_2(\chi\chi)_2)_{1_1} && I_5^{\chi_R} = (\chi_R\chi)_{1_1}\sigma\sigma \\
&I_3^{\chi_R} = ((\chi_R\chi)_{3_1}(\chi\chi)_{3_1})_{1_1} && \\
&I_1^{D_R} = ((D_R\chi)_{3_1}(\varphi\varphi')_{3_1})_{1_1} && I_4^{D_R} = (D_R(\varphi\varphi)_2)_{1_1}\,\sigma \\
&I_2^{D_R} = ((D_R\chi)_{3_2}(\varphi\varphi')_{3_2})_{1_1} && I_5^{D_R} = (D_R(\varphi'\varphi')_2)_{1_1}\,\sigma \\
&I_3^{D_R} = ((D_R\chi)_{3_1}(\varphi'\varphi')_{3_1})_{1_1} && I_6^{D_R} = (D_R(\varphi\varphi')_2)_{1_1}\,\sigma \\
&I_1^{\varphi_R} = (\varphi_R\chi)_{1_s}(\varphi\varphi')_{1_2} && I_4^{\varphi_R} = ((\varphi_R\chi)_{3_2}(\varphi\varphi')_{3_2})_{1_1} \\
&I_2^{\varphi_R} = ((\varphi_R\chi)_2(\varphi\varphi')_2)_{1_1} && I_5^{\varphi_R} = (\varphi_R(\varphi\varphi')_{3_2})_{1_1}\,\sigma \\
&I_3^{\varphi_R} = ((\varphi_R\chi)_{3_1}(\varphi\varphi')_{3_1})_{1_1} \ . &&
\end{aligned} \tag{4.B.3}$$

In these terms we indicate with $(\ldots)_R$ the representation R of S_4.

The NLO flavon vevs are obtained by imposing the vanishing of the first derivative of $w_d + \delta w_d$ with respect to the driving fields σ_R, χ_R, D_R and φ_R. We look for a solution that perturbs equations (4.16) and (4.17) to first order in the $1/\Lambda$ expansion: for all components of the flavons $\Phi = (\sigma,\ \chi,\ \varphi,\ \varphi')$, we denote the shifted vev's by

$$\langle \Phi \rangle = \langle \Phi \rangle_{LO} + \delta\Phi \ . \tag{4.B.4}$$

The original $\langle \Phi \rangle_{LO}$ here are given by equations (4.16) and (4.17).

It is straightforward to verify the following results. In the Majorana mass sector the shifts $\delta\sigma,\ \delta\chi$ turn out to be proportional to the LO vev's $\langle \Phi \rangle_{LO}$ and can be absorbed in a redefinition of the parameters v_χ and v_σ. Instead, in the Dirac mass sector, the shifts $\delta\varphi,\ \delta\varphi'$ have a non-trivial structure, so that the LO texture is modified:

$$\langle \varphi \rangle = \begin{pmatrix} \delta v_\varphi \\ v'_\varphi \\ v'_\varphi \end{pmatrix} \qquad \langle \varphi' \rangle = \begin{pmatrix} \delta v_{\varphi'} \\ v'_{\varphi'} \\ -v'_{\varphi'} \end{pmatrix} \ . \tag{4.B.5}$$

Here v'_φ and $v'_{\varphi'}$ satisfy a relation similar to that in equation (4.72) and the shifts δv_φ and $\delta v_{\varphi'}$ are suppressed by a factor λ with respect to the LO entries v'_φ and $v'_{\varphi'}$, respectively.

4.C Beta coefficients of the gauge coupling running

In this appendix, we provide the coefficients of the β–functions for the gauge coupling running in the different regimes. The complete matter fields run from the GUT scale down to the M_{SUSY} scale, where the SUSY partners decouple. We have already outlined the spectrum for the scalar fields in section 4.9, according to the different scale at which the fields decouple. As a result the computation of the β–functions is straightforward. We write μ for a generic scale and obtain in the different energy regimes

- $M_C < \mu < M_{GUT}$: all matter is in the left and right handed multiplets $(4,\ 2,\ 1)$ and $(\overline{4},\ 1\,,2)$ as mentioned in table 4.2. In the Higgs sector, we have all the fields mentioned in table 4.6. This leads to the coefficients

  $$\beta_{SU(4)_C} = 54 \ , \qquad \beta_{SU(2)_L} = 69 \ , \qquad \beta_{SU(2)_R} = 69 \ . \tag{4.C.1}$$

  Due to the large matter content these coefficients are very large and the β–functions are very steep. As consequence the theory is in the Pati-Salam regime only for a very small range of energies, as can indeed be seen in figure 4.8. Almost directly after passing the scale M_C, the $SU(2)_R$ coupling constant enters the non-perturbative regime.

- $M_R < \mu < M_C$: in this range the Pati-Salam gauge group is broken to the 'colour-broken Pati-Salam' $SU(3)_C \times SU(2)_L \times SU(2)_R \times U(1)_{B-L}$ symmetry. We find the following coefficients for the matter (left and right handed doublets of quarks and leptons characterized by different $U(1)_{B-L}$ charges) and the scalar fields

  $$\beta_{SU(3)_C} = -3 \ , \qquad \beta_{SU(2)_L} = 18 \ , \qquad \beta_{SU(2)_R} = 18 \ , \qquad \beta_{U(1)_{B-L}} = 24 \ . \tag{4.C.2}$$

- $M_T < \mu < M_R$: in this regime we have all the usual MSSM matter particles, four light higgs doublets (two up-type and two down-type), a couple of SM triplets $(1,3,1) \oplus (1,3,-1)$ and two extra charged singlets (δ^{++} and $\bar{\delta}^{++}$). The coefficients of the β–functions are

  $$\beta_{SU(3)_C} = -3 \ , \qquad \beta_{SU(2)_L} = 4 \ , \qquad \beta_{U(1)_Y} = 69/5 \ . \tag{4.C.3}$$

  The hypercharge that appears in the last term is related to $SU(2)_R$ and the $B-L$ charges in the previous regime by

  $$Y = T_{3R} + \frac{B-L}{2}.$$

- $M_{SUSY} < \mu < M_T$: in this regime we have all the usual MSSM matter particles, four light higgs doublets (two up-type and two down-type) and two extra charged singlets (δ^{++} and $\bar{\delta}^{++}$). The β–function coefficients are

$$\beta_{SU(3)_C} = -3\,, \qquad \beta_{SU(2)_L} = 2\,, \qquad \beta_{U(1)_Y} = 12\,. \tag{4.C.4}$$

  This should be compared with the (-3, 1, 33/5) coefficients of the ordinary MSSM.

- $v_W < \mu < M_{SUSY}$: we have the particle content of the standard model, with the exception that there are four Higgs doublets. We have therefore the following β–function coefficients

$$\beta_{SU(3)_C} = -7\,, \qquad \beta_{SU(2)_L} = -8/3\,, \qquad \beta_{U(1)_Y} = 22/5\,. \tag{4.C.5}$$

  This should be compared with the (-7, -19/6, 41/10) coefficients of the ordinary SM.

4.D Yukawa running

In section 2.1.1 we remarked that we can consider only the running between M_T and M_{SUSY} to provide analytical approximations for the evolution of fermion masses and mixing under the RGEs effect. This is due to the closeness of the intermediate scales between M_{GUT} and M_T. At M_T the scalar $SU(2)_L$ triplet has been already integrated out giving rise to the effective Weinberg operator for neutrino masses

$$\alpha_{ij} Y_{L_{rs}} \frac{L_r L_s h_{u_i} h_{u_j}}{M_T}\,, \tag{4.D.1}$$

For the Higgs fields we have $h_{u_1} = h_u$ and $h_{u_2} = h'_u$; the α_{ij} coefficients arise from the scalar potential and Y_L is given in equation (4.80).

For what concerns the charged fermion Yukawa, at M_T the Dirac part of the superpotential is written as

$$Y_u Q\, U^c h_u + Y'_u Q\, U^c h'_u + Y_d Q\, D^c h_d + Y'_d Q\, D^c h'_d + Y_e L\, E^c h_d + Y'_e L\, E^c h'_d\,, \tag{4.D.2}$$

with the Yukawa mass matrices given in equation (4.82).

The Yukawa matrices RGEs are therefore given by

$$\begin{aligned}
16\pi^2 \frac{dY_u}{dt} &= \left[3\,Y_u Y_u^\dagger + Y_d Y_d^\dagger + 3\,Y'_u Y'^\dagger_u + Y'_d Y'^\dagger_d + 3\,\mathrm{Tr}(Y_u Y_u^\dagger) - \Sigma_i c_i^u g_i^2\right] Y_u\,,\\
16\pi^2 \frac{dY'_u}{dt} &= \left[3\,Y_u Y_u^\dagger + Y_d Y_d^\dagger + 3\,Y'_u Y'^\dagger_u + Y'_d Y'^\dagger_d + 3\,\mathrm{Tr}(Y'_u Y'^\dagger_u) - \Sigma_i c_i^u g_i^2\right] Y'_u\,,\\
16\pi^2 \frac{dY_d}{dt} &= \left[Y_u Y_u^\dagger + 3\,Y_d Y_d^\dagger + Y'_u Y'^\dagger_u + 3\,Y'_d Y'^\dagger_d + 3\,\mathrm{Tr}(Y_d Y_d^\dagger) + \mathrm{Tr}(Y_e Y_e^\dagger) - \Sigma_i c_i^d g_i^2\right] Y_d\,,\\
16\pi^2 \frac{dY'_d}{dt} &= \left[Y_u Y_u^\dagger + 3\,Y_d Y_d^\dagger + Y'_u Y'^\dagger_u + 3\,Y'_d Y'^\dagger_d + 3\,\mathrm{Tr}(Y'_d Y'^\dagger_d) + \mathrm{Tr}(Y'_e Y'^\dagger_e) - \Sigma_i c_i^d g_i^2\right] Y'_d\,,\\
16\pi^2 \frac{dY_e}{dt} &= \left[3\,Y_e Y_e^\dagger + 3\,Y'_e Y'^\dagger_e + 3\,\mathrm{Tr}(Y_d Y_d^\dagger) + \mathrm{Tr}(Y_e Y_e^\dagger) - \Sigma_i c_i^e g_i^2\right] Y_e\,,\\
16\pi^2 \frac{dY'_e}{dt} &= \left[3\,Y_e Y_e^\dagger + 3\,Y'_e Y'^\dagger_e + 3\,\mathrm{Tr}(Y'_d Y'^\dagger_d) + \mathrm{Tr}(Y'_e Y'^\dagger_e) - \Sigma_i c_i^e g_i^2\right] Y'_e\,,\\
16\pi^2 \frac{dY_L}{dt} &= \left[(Y_e Y_e^\dagger + Y'_e Y'^\dagger_e) Y_L + Y_L (Y_e Y_e^\dagger + Y'_e Y'^\dagger_e)^T - \Sigma_i c_i^\nu g_i^2) Y_L\right] (\alpha_{11} + \alpha_{12} + \alpha_{22})\\
&\quad + \left[6\,\mathrm{Tr}(Y_u Y_u^\dagger)\alpha_{11} + 3\,\mathrm{Tr}(Y_u Y_u^\dagger)\alpha_{12} + 3\,\mathrm{Tr}(Y'_u Y'^\dagger_u)\alpha_{12} + 6\,\mathrm{Tr}(Y'_u Y'^\dagger_u)\alpha_{22}\right] Y_L\,,
\end{aligned} \tag{4.D.3}$$

The coefficients here are numerically given by

$$\begin{aligned} c_1^u &= \frac{13}{15}\,, \qquad c_2^u = 3\,, \qquad c_3^u = \frac{16}{3}\,, \qquad & c_1^d &= \frac{7}{15}\,, \qquad c_2^d = 3\,, \qquad c_3^d = \frac{16}{3}\,, \\ c_1^e &= \frac{9}{5}\,, \qquad c_2^e = 3\,, \qquad c_3^e = 0\,, \qquad & c_1^\nu &= \frac{6}{5}\,, \qquad c_2^\nu = 6\,, \qquad c_3^\nu = 0\,. \end{aligned} \tag{4.D.4}$$